G, Lo 11

HYDROMETEOROLOGICAL REPORT NO. 24

MAXIMUM POSSIBLE PRECIPITATION SAN JOAQUIN BASIN, CALIFORNIA

WASHINGTON
July 1947

HYDROMETEOROLOGICAL REPORTS

(Nos. 6–22 numbered retroactively)

No. 1 Maximum possible precipitation over the Ompompanoosuc Basin above Union Village, Vermont. 1943.

No. 2 Maximum possible precipitation over the Ohio River Basin above Pittsburgh, Pennsylvania. 1942.

No. 3 Maximum possible precipitation over the Sacramento Basin of California. 1943.

No. 4 Maximum possible precipitation over the Panama Canal Basin. 1943.

No. 5 Thunderstorm rainfall. 1947.

No. 6 A preliminary report on the probable occurrence of excessive precipitation over Fort Supply Basin, Oklahoma. 1938.*

No. 7 Worst probable meteorological condition on Mill Creek, Butler and Hamilton Counties, Ohio. 1937. (Unpublished.) Supplement, 1938.*

No. 8 A hydrometeorological analysis of possible maximum precipitation over St. Francis River Basin above Wappapello, Missouri. 1938.*

No. 9 A report on the possible occurrence of maximum precipitation over White River Basin above Mud Mountain Dam site, Washington. 1939.*

No. 10 Maximum possible rainfall over the Arkansas River Basin above Caddoa, Colorado. 1939.* Supplement, 1939.*

No. 11 A preliminary report on the maximum possible precipitation over the Dorena, Cottage Grove, and Fern Ridge Basins in the Willamette Basin, Oregon. 1939.*

No. 12 Maximum possible precipitation over the Red River Basin above Denison, Texas. 1939.*

No. 13 A report on the maximum possible precipitation over Cherry Creek Basin in Colorado. 1940.*

No. 14 The frequency of flood producing rainfall over the Pajaro River Basin in California. 1940.*

No. 15 A report on depth-frequency relations of thunderstorm rainfall on the Sevier Basin, Utah. 1941.*

No. 16 A preliminary report on the maximum possible precipitation over the Potomac and Rappahannock River Basins. 1943.*

No. 17 Maximum possible precipitation over the Pecos Basin of New Mexico. 1944. (Unpublished.)

No. 18 Tentative estimates of maximum possible flood-producing meteorological conditions in the Columbia River Basin. 1945.

No. 19 Preliminary report on depth-duration-frequency characteristics of precipitation over the Muskingum Basin for one to nine week periods. 1945.*

No. 20 An estimate of maximum possible flood-producing meteorological conditions in the Missouri River Basin above Garrison Dam site. 1945.

No. 21 A hydrometeorological study of the Los Angeles area. 1939.*

No. 21A Preliminary report on maximum possible precipitation, Los Angeles area, California. 1944.*

No. 21B Revised report on maximum possible precipitation, Los Angeles area, California. 1945.

No. 22 An estimate of maximum possible flood-producing meteorological conditions in the Missouri River Basin between Garrison and Fort Randall. 1946.

No. 23 Generalized estimates of maximum possible precipitation over the United States east of the 105th meridian, for areas of 10, 200, and 500 square miles. 1947.

* Out of print.

U.S. Department of Commerce
Weather Bureau

U.S. War Department
Corps of Engineers

Hydrometeorological Report No. 24

MAXIMUM POSSIBLE PRECIPITATION

OVER THE SAN JOAQUIN BASIN, CALIFORNIA

Prepared by
The Hydrometeorological Section
Division of Climatological and Hydrologic Services
U.S. Weather Bureau

Washington
July 1947

SAN JOAQUIN RIVER BASIN
CALIFORNIA

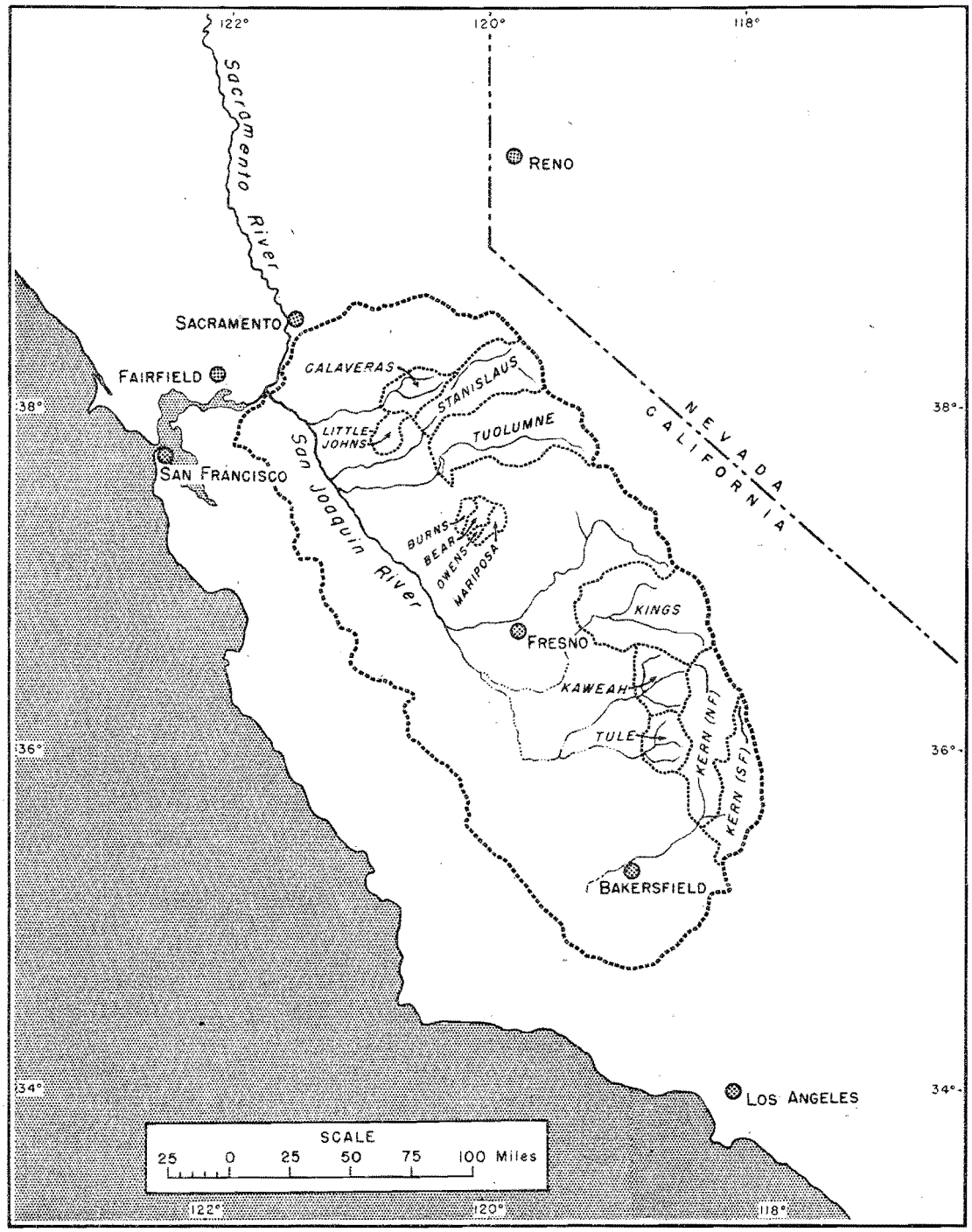

CONTENTS

CONTENTS
(cont.)

TABLES

TABLES
(cont.)

FIGURES

FIGURES
(cont.)

I

INTRODUCTION

Assignment

1. An estimate of the maximum possible precipitation and accompanying snow melt over the San Joaquin Basin of California, and its sub-basins, was undertaken by the Hydrometeorological Section in response to a request dated April 11, 1946, from the Office of the Chief of Engineers, War Department. In accordance with agreement in conference, preliminary values of precipitation and snow melt for the San Joaquin as a whole, the Kings River above Pine Flat, and the Kern River above Isabella were provided the Engineers on August 19, 1946. Revised precipitation values for the latter two basins, forwarded to the Engineers on December 4, 1946, are retained in the final report but the snow-melt estimates have been changed. Basins considered in this report are as follows:

Basin	Area (sq. mi.)
San Joaquin	35,524
Kern River above Isabella Dam site Kern, North Fork - 1070 sq. mi. Kern, South Fork - 1010 sq. mi.	2080
Kings River above Pine Flat Dam site	1542
Tuolumne River above New Don Pedro Dam site	1536
Stanislaus River above New Melones Dam site	900
Kaweah River above Terminus Dam site	560
Tule River above Success Dam site	417
Calaveras River above Hogan Dam site	363
Littlejohns Creek above Farmington Dam site	212

Mariposa Creek above Mariposa Dam site	108
Burns Creek above Burns Dam site	74
Bear Creek above Bear Dam site	72
Owens Creek above Owens Dam site	25.6

Background

2. The primary problem in the San Joaquin is that of orographic precipitation. Two previous Section reports, for the Sacramento Basin [1/] and for the Los Angeles area [2/], have treated the same problem.

3. In the Sacramento Report the storage principle was applied to the computation of the rainfall. The flow model used was that of a hypothetical thunderstorm cell, on the assumption that each column of air crossing the basin would be forced to release the precipitation equivalent of a certain amount of convective overturning. The vertical dimensions of the cell were made direct functions of sea-level (1000 mb) dewpoint, and the depleting effect of an inflow barrier a direct function of the barrier height. Despite the simplifications involved in the model, it was possible to reproduce total-basin depth-duration values by substituting key-station wind speeds and dewpoints in the rainfall equation formulated.

4. A more realistic approach was developed in the Los Angeles Report. Although the storage principle was retained, the convective cell was abandoned in favor of an orographic model compatible with the major topographic features of the area. Variables measuring changes in wind direction and percentage of area exposed to up-slope winds were introduced, and an empirical coefficient varying with sea-level (1000 mb) dewpoint developed.

1/ References listed numerically at end of report.

Substitution of observed values of the variables in the final formula made possible the reproduction of the observed mass curves of rainfall over the 10,000-square-mile area of maximum rainfall in the major storms.[3]

5. A statistical approach to the computation of orographic rainfall is being investigated by G. Platzman of the Portland Engineer District. It is based on the extrapolation of statistical relationships established between index-station wind and dewpoint measurements, and the accompanying 12-hour major-storm rainfall in the Willamette Basin of Oregon.

San Joaquin Method

6. The severely limited record of major storms in the San Joaquin Basin and the inadequacy of both meteorological and rainfall observations in the recorded storms made necessary a somewhat more theoretical approach than in any of the foregoing studies. Preliminary review of the literature on orographic precipitation disclosed no substantial advances after Pockels' early treatise[3/], in which he computed fields of motion over barriers of various shapes and sizes, assuming steady-state frictionless flow in a two-dimensional system in thermodynamically neutral equilibrium. However, his numerical results, based on the extremely sketchy upper-air data of the period, were too uncertain for application. The Section's approach has been, in the main, to add to the proven results of earlier reports the refinements made possible by utilization of new upper-air storm-wind data and the empirical-theoretical modifications necessary to the computation for the smaller basins.

7. Because tests had shown both the Sacramento and the Los Angeles methods adequate for the computation of long-duration, large-areal rainfall in their respective regions, each method was in turn applied to the San Joaquin, which lies between the two regions. Agreement in the results

4 of these computations indicated the acceptability of either solution for the maximum possible 66-hour storm over the San Joaquin Basin as a whole.

8. Application to the smaller basins required a change in technique because of the inadequacy of the earlier methods for such a computation. Availability of upper-air rawin observations in the important San Joaquin storm of January 30-February 3, 1945 (not available for the earlier reports) made possible the formulation of an expression for orographic precipitation more suitable for small-basin computation. On a theoretical basis, the effect of spillover, of increasing importance with decrease of basin length along the wind, was introduced into the computation. On an empirical basis, the effect of pre-barrier, upwind lift was also evaluated. For the basins lying at elevations below the Coast Range barriers, and therefore not amenable to the purely orographic treatment, maximum precipitation values were determined through relations obtained from observed distributions within the major storms in the region.

9. In addition to the usual data analyzed in order to determine the snow-melt contribution to the runoff from the maximum storm, basic day-to-day data furnished by Cooperative Snow Investigations were processed by the Section. The results, especially in view of the short record available, did not justify at this time a change from the formula developed by Light[4/] for previous reports.

Acknowledgments

10. S. B. Solot, project leader, was mainly responsible for the new approaches introduced in the report. A. L. Shands was supervising editor, assisted by H. C. Hamilton. Principal contributors, in addition to Mr. Solot, were A. M. Kahan, N. E. Manos, T. J. Nordenson, and R. W. Schloemer, with technical assistance furnished by G. D. Abrams, D. Ammerman, J. C.

Coffin, J. H. Cornish, H. K. Gold, E. S. Thompson, and M. M. Webster. W. E. Kinnear was in charge of drafting. Special advice on the snow-melt problem was furnished by P. Light, then Regional Engineer at Seattle, and W. T. Wilson, Chief of the Processing and Analysis Unit of Cooperative Snow Investigations. C. Schneider, of the Sacramento District Engineer Office, detailed to the Section for several months in the early stages of the project, gave important assistance in the clarification of the District's special needs and problems in the San Joaquin Basin.

II

THE BASIN-WIDE MAXIMUM POSSIBLE STORM

Storm Type

11. The flood-producing storms of the Pacific Coast are discussed at length in the Sacramento Report and further remarks, applying specifically to the Southern California Coast, appear in the Los Angeles Report. Detailed discussion of Pacific Coast synoptic types may be found in papers by Reed [5] and Brown [6]. It can be concluded from these discussions that there are no great differences in type between the maximum possible storms affecting any of the larger basins in the Coastal States. The storms which are most critical on a large scale all have a strong west-to-east zonal flow associated with deep cyclonic centers offshore. The location of the cyclonic center and the variation of inflow direction between west and south determine the general location of the heaviest precipitation. Distribution of the heavy precipitation within the area depends on the orientation of topographic features.

12. Comparison of the record general storms over the Sacramento and the San Joaquin, the storms of December 9-12, 1937, and January 30-February 3, 1945, respectively, shows no important differences except an inflow wind from a more westerly direction in the 1945 storm. Whereas SW was found to be the most critical inflow direction for Sacramento storms, WSW, as will be shown later, was found to be the most critical for the San Joaquin. Comparison of the 1945 storm with the record general storm over the Los Angeles area, January 19-24, 1943, shows somewhat greater differences. The location of the cyclonic center was farther south in the 1943

storm and the prevailing inflow direction was more nearly SSW - the most critical for the Los Angeles area.

13. The essential similarity of these storms, each the prototype of the maximum possible storm over its region, plus the fact that the San Joaquin Basin lies between the Sacramento and Los Angeles areas, justifies the assumption that the meteorological sequence in the San Joaquin maximum storm will closely resemble the sequences in the maximum storms for the other areas. It follows that, by use of appropriate empirical constants - specific to the topographic character of the San Joaquin, the maximum possible precipitation over either the Sacramento Basin or the Los Angeles area could be transposed and adjusted for an estimate of the maximum possible precipitation over the San Joaquin. In the absence of such constants, a more direct approach is required, namely, the computation of the maximum possible precipitation over the San Joaquin by applying combinations of Sacramento and Los Angeles models and meteorological sequences to the San Joaquin Basin. Such a procedure, described in detail in the following sections, yields an average depth of 11.9 inches in 66 hours as the maximum possible precipitation over the San Joaquin Basin.

Sacramento and Los Angeles Maximum Storms

14. To facilitate the application of the Sacramento and Los Angeles maximum-storm data to the San Joaquin, each storm was defined by three variables: wind direction, total inflow-wind movement for 66 hours, and an average 66-hour dewpoint. In each case the wind was assumed constant throughout the storm at its optimum direction, i.e., 225° in the Sacramento storm and 210° in the Los Angeles storm. The average dewpoint was the 1000-mb dewpoint corresponding (in the moisture-storage equation)

[8] to the average depth of basin or areal rainfall per mile of inflow-wind movement. It was obtained by dividing total inflow-wind movement into total rainfall and entering with the quotient (and the optimum direction) into table 33 of the Sacramento Report or figure 8 of the Los Angeles Report. By the maximum possible storm for a particular area, then, is meant the combination of the three meteorological variables - inflow-wind movement, average dewpoint, and wind direction - which produces the maximum possible precipitation over that area. Transposed to another area, the same combination of wind and dewpoint may yield an entirely different value of precipitation. In the two maximum storms considered, the pertinent values are:

Table 1

SACRAMENTO AND LOS ANGELES MAXIMUM POSSIBLE STORMS (66 HOURS)

	Precip - R (inches)	Wind - Vt (miles)	R/Vt (inches/mile)	Dewpoint (^{o}F)	Optimum Wind Dir.
Sacramento	10.8	3036	.00356	60	225^{o}
Los Angeles	17.1	4000	.00427	55	210^{o}

The difference between the average dewpoints of table 1 is not a difference in actual or maximum dewpoint. There is, in the first place, a weighting by wind in the computation of the average dewpoint of the table. In the second place, the use, in the Los Angeles Report, of a moisture coefficient $f(T_D)$ and a percentage of area exposed to up-slope wind, tends to reduce the computed dewpoint.

15. To abbreviate the discussion the following symbols are used:

MPS - Maximum possible storm, i.e., combination of wind and dewpoint producing maximum possible precipitation

MPP - Maximum possible precipitation

T_{LA} - Los Angeles theoretical model or formula

T_{LA1} - Adaptation of T_{LA} with constant nodal surface

T_{LA2} - Adaptation of T_{LA} with nodal surface higher at outflow than at inflow barrier

T_{SAC} - Sacramento theoretical model or formula

S_{LA} - Los Angeles MPS

S_{SAC} - Sacramento MPS

R_{LA} - Rainfall over the Los Angeles area derived by use of T_{LA}

R_{SAC} - Rainfall over the Sacramento Basin derived by use of T_{SAC}

R_{SJ} - Rainfall over the San Joaquin Basin

The nodal surface is defined as the surface above which the atmosphere remains undisturbed by the effects of the orographic barrier.

Application of Los Angeles Storm and Theory

16. As stated in the Los Angeles Report, T_{LA} applies to a one-barrier model. For application to the San Joaquin it must be adapted to two barriers, one at inflow as well as one at outflow. Since the height of the San Joaquin outflow barrier is considerably greater than either the San Joaquin inflow or the Los Angeles outflow barrier, and since both theory and experience indicate a variation of nodal-surface height with barrier height, a further adaptation of T_{LA} was required. Thus, two possible adaptations were assumed for the San Joaquin computation. In T_{LA1} the nodal surface was kept at 460 mb at both inflow and outflow barriers; in T_{LA2} the nodal surface was raised to 300 mb at the outflow barrier but kept at 460 mb at the inflow barrier. The two models are illustrated in figure 1.

17. The only difference between T_{LA} and T_{LA1} is the insertion of an inflow barrier in the latter model. Using subscripts 1, 2, and 3 to refer to conditions before the inflow barrier, at the inflow barrier, and at the outflow barrier, respectively, the equation for T_{LA} states:

$$R = \frac{\bar{f}\,\bar{V}_1\,t}{Y}\left(W_1 - \frac{\Delta p_1}{\Delta p_3}\,W_3\right) \tag{1}$$

where

R is average depth of precipitation in basin

$\bar{f}$ is an empirical function of dewpoint

$\bar{V}_1\,t$ is total wind movement (4000 miles in table 1)

Y is length of basin parallel to wind direction

W is precipitable water between nodal surface and ground surface

Δp is pressure difference between nodal surface and ground surface

18. The rainfall produced by the inflow barrier can also be stated in the T_{LA} form

$$R = \frac{\bar{f}\,\bar{V}_1\,t}{Y}\left(W_1 - \frac{\Delta p_1}{\Delta p_2}W_2\right) \tag{2}$$

Subtracting (2) from (1) gives the two-barrier equation for T_{LA1}:

$$R = \frac{\bar{f}\,\bar{V}_1\,t}{Y}\left(\frac{\Delta p_1}{\Delta p_2}W_2 - \frac{\Delta p_1}{\Delta p_3}W_3\right) \tag{3}$$

19. Similarly, then, for T_{LA2}:

$$R = \frac{\bar{f}\,\bar{V}_1\,t}{Y}\left[\left(W_1' - \frac{\Delta p_1'}{\Delta p_3'}\,W_3'\right) - \left(W_1 - \frac{\Delta p_1}{\Delta p_2}W_2\right)\right] \tag{4}$$

Where W_1' and $\Delta p_1'$ refer, respectively, to the precipitable water and pressure difference between the second, higher nodal surface and 1000 mb; and W_3' and $\Delta p_3'$ refer to the precipitable water and pressure difference between the second nodal surface and the top of the second or outflow

barrier. (The assumption is made that $\bar{V}_1$ for the layer to 300 mb equals $\bar{V}_1$ for the layer to 460 mb.) [11]

20. Equation (1) can be applied to the Los Angeles area, equations (3) and (4) to the San Joaquin Basin. For the same storm, $\bar{f}\,\bar{V}_1\,t$ will have the same value in all three computations. All other values will be specific to the Los Angeles area in (1) and to the San Joaquin Basin in (3) and (4). The Los Angeles and San Joaquin equations can then be combined as follows:

(By T_{LA1})

$$R_{SJ} = R_{LA}\left(\frac{Y}{W_1 - \frac{\Delta p_1}{\Delta p_3} W_3}\right)_{LA}\left(\frac{\frac{\Delta p_1}{\Delta p_2} W_2 - \frac{\Delta p_1}{\Delta p_3} W_3}{Y}\right)_{SJ} \qquad (5)$$

(By T_{LA2})

$$R_{SJ} = R_{LA}\left(\frac{Y}{W_1 - \frac{\Delta p_1}{\Delta p_3} W_3}\right)_{LA} \cdot \left[\frac{\left(W_1' - \frac{\Delta p_1'}{\Delta p_3'} W_3'\right) - \left(W_1 - \frac{\Delta p_1}{\Delta p_2} W_2\right)}{Y}\right]_{SJ} \qquad (6)$$

21. Evaluation of the quantities inside the first parenthesis (the LA factor) results in

$$\frac{60}{1.046 - \frac{540}{340}(0.440)} = 172.9 \text{ miles/inch}$$

A fixed wind direction is assumed in this computation. In evaluating the second parenthesis in each equation (the SJ factor), several wind directions in the SW quadrant were assumed. Later, a decision was made concerning which of these directions should be used in the maximum possible storm over the San Joaquin. The computed SJ factors ($\times 10^5$) are:

	S	SW	WSW	W
T_{LA1}	48	296	323	305
T_{LA2}	100	385	414	390

The individual values involved in these computations are listed in table 2.

Table 2

SAN JOAQUIN (T_{LA}) VALUES

	S	SW	WSW	W
Pressure at inflow (mb)	844	879	896	906
Height at inflow (ft)	4680	3700	3100	2750
Pressure at outflow (mb)	779	679	684	693
Height at outflow (ft)	7180	10,150	10,240	9950
Y (miles)	151.4	113.6	111.1	117.4
Δp_1 (mb)	540	540	540	540
$\Delta p_1'$ (mb)	700	700	700	700
Δp_2 (mb)	384	419	436	446
Δp_3 (mb)	319	219	224	233
$\Delta p_3'$ (mb)	479	379	384	540
W_1 (in.)	1.046	1.046	1.046	1.046
W_1' (in.)	1.074	1.074	1.074	1.074
W_2 (in.)	0.524	0.647	0.698	0.728
W_3 (in.)	0.392	0.202	0.210	0.226
W_3' (in.)	0.420	0.230	0.238	0.254

22. Outflow and inflow barriers were computed as in the Sacramento Report. On a large-scale topographic map, parallel lines were drawn across the basin at 5-mile intervals along each of the directions used. Inflow and outflow barrier heights were estimated to the nearest 1000 feet within each strip and the length of each strip measured to the nearest mile for the Y computation. Barrier heights were converted to

pressures on the assumption of a sea-level temperature of 55 F (the S_{LA} 66-hour average dewpoint, from table 1) at 1000 mb in a saturated atmosphere with pseudo-adiabatic lapse rate. Mean pressures and basin lengths were then computed.

23. Substituting an R_{LA} value of 17.1 inches (table 1) in equations (5) and (6), and using the appropriate computed values of the LA and SJ factors, the values of estimated 66-hour MPP over the San Joaquin Basin become:

	S	SW	WSW	W
T_{LA1}	1.4	8.8	9.5	9.0
T_{LA2}	3.0	11.4	12.2	11.5

Application of Sacramento Storm and Theory

24. The T_{SAC} rainfall equation is

$$R = \frac{\bar{W}_E \, \bar{V} \, t \, \bar{L}}{Y} \qquad (7)$$

where

$\bar{W}_E$ is mean weighted effective precipitable water, a function of dewpoint

$\bar{V}$ t is total wind movement (3036 miles in table 1)

$\bar{L}$ is mean weighted lift coefficient, a function of inflow-barrier height and dewpoint

25. The same equation can be applied to the San Joaquin. In the same storm the value $\bar{W}_E \, \bar{V}$ t will be constant, while $\bar{L}$ and Y will have specific values in each basin. The equation can thus be combined into

$$R_{SJ} = R_{SAC} \frac{(\bar{L}/Y)_{SJ}}{(\bar{L}/Y)_{SAC}} \qquad (8)$$

26. In table 31 of the Sacramento Report, $\bar{L}$ for a dewpoint of 63 F, SW direction, is 0.63. With this as an argument in figure 18 of the

Sacramento Report, $\bar{L}$ for 60 F (the S_{SAC} 66-hour average dewpoint) is found to be 0.61. Y for a SW direction of inflow over the Sacramento is 117 miles. Thus, $(\bar{L}/Y)_{SAC}$, the SAC factor, becomes

$$\frac{0.61}{117} = 521 \times 10^{-5} \text{ mi}^{-1}$$

27. To compute the SJ factor, the inflow-barrier heights available in table 2 were used as arguments in finding the appropriate $\bar{L}$ for 60 F in figure 18 of the Sacramento Report. The values of Y are also available in table 2. The necessary values and the computed SJ factors are contained in table 3, below.

Table 3

SAN JOAQUIN (T_{SAC}) VALUES

	S	SW	WSW	W
Inflow height H (ft)	4680	3700	3100	2750
$\bar{L}$	0.51	0.59	0.64	0.68
Y (miles)	151.4	113.6	111.1	117.4
$(\bar{L}/Y)_{SJ} \times 10^5$ (mi^{-1})	337	519	576	575

28. Using an R_{SAC} value of 10.8 inches (table 1), the estimated 66-hour MPP values over the San Joaquin Basin become:

	S	SW	WSW	W
T_{SAC}	7.0	10.8	11.9	11.9

Application of Storm and Theory Combinations

29. To complete the possible applications of storm and theory to the San Joaquin, it was also desirable to compute the San Joaquin MPP on the basis of a combination of S_{SAC} and T_{LA} and also of S_{LA} and T_{SAC}. To a close approximation, equations (5), (6), and (8), and the LA, SJ, and SAC factors already computed for them, can still be used if a new R_{LA} is

derived from a combination of S_{SAC} and T_{LA}, and a new R_{SAC} from a combination of S_{LA} and T_{SAC}.

30. Based on equation (1), the computation of the original R_{LA} involved an integration with respect to time. This procedure was repeated in the computation of the new R_{LA} resulting from a combination of S_{SAC} and T_{LA}. The integration is shown in table 4.

Table 4

COMPUTATION OF R_{LA} (S_{SAC}, T_{LA})

Time (hours)	f x 10^4 (inches)	Wind Movement (miles)	Precip (inches)
0-6	26	222	0.58
6-12	42	246	1.03
12-18	54	270	1.46
18-24	62	288	1.79
24-30	68	312	2.12
30-36	71	366	2.60
36-42	68	312	2.12
42-48	62	282	1.79
48-54	54	270	1.46
54-60	42	246	1.03
60-66	26	222	0.58
0-66			16.56

31. To obtain the new R_{SAC}, based on equation (7), the moisture index f (where $f = K W_E$ and $K = \frac{5\Sigma L}{\text{area}}$) corresponding to the Sacramento optimum wind direction, SW, and to the 66-hour average S_{LA} dewpoint, 55 F, was obtained from table 33 of the Sacramento Report and multiplied by the S_{LA} total wind movement:

$$.0027 \times 4000 = 10.8 \text{ inches}$$

This was essentially the manner in which R_{SAC} was originally computed.

32. Summarizing all 66-hour R_{LA} and R_{SAC} values used:

$$R_{LA}\ (T_{LA},\ S_{LA}) = 17.1 \text{ inches}$$

$$R_{LA}\ (T_{LA},\ S_{SAC}) = 16.6 \text{ inches } *$$

$$R_{SAC}\ (T_{SAC},\ S_{SAC}) = 10.8 \text{ inches}$$

$$R_{SAC}\ (T_{SAC},\ S_{LA}) = 10.8 \text{ inches } *$$

The unstarred values have already been used in equations (5), (6), and (8) in computing MPP_{SJ}, for the combination T_{LA} and S_{LA} and for the combination T_{SAC} and S_{SAC}. The starred values can now be used in the same equations to compute MPP_{SJ} for the storm and theory combinations indicated. The results of all the computations are summarized in table 5.

Table 5

ESTIMATED 66-HOUR MAXIMUM POSSIBLE PRECIPITATION
SAN JOAQUIN BASIN

Wind Directions	S	SW	WSW	W
S_{LA}, T_{LA1}	1.4	8.8	9.5	9.0
S_{LA}, T_{LA2}	3.0	11.4	12.2	11.5
S_{LA}, T_{SAC}	7.0	10.8	11.9	11.9
S_{SAC}, T_{LA1}	1.4	8.5	9.3	8.7
S_{SAC}, T_{LA2}	2.9	11.1	11.9	11.2
S_{SAC}, T_{SAC}	7.0	10.8	11.9	11.9

San Joaquin Maximum Possible Precipitation

33. Examination of table 5 shows the WSW direction of inflow to be the most productive, or as productive as any of the other directions, no matter what combination of storm and theory is used. Synoptic analysis of the major storms in the region shows WSW to be the most critical direction. Also, it is significant that T_{LA1} produces the lowest values for each of the directions. This is to be expected, since the method neglects

the variation, indicated by both theory and experience, of nodal height with barrier height.

34. Consideration of these facts confines the most acceptable values in the table to those under the direction WSW and to those in lines 2, 3, 5, and 6. These values have been underlined. The value 11.9 has been chosen as the best estimate of the maximum possible 66-hour precipitation over the San Joaquin Basin as a whole, partly because of its prominence by repetition. The choice is better justified by the fact that San Joaquin storms resemble the Sacramento type most closely, and both acceptable S_{SAC} derived values are 11.9. The physical characteristics of the two basins also resemble each other closely. However, all West Coast storms are so similar in character that S_{LA} is by no means excluded as a possibility.

35. Table 5 also offers the opportunity to compare the Los Angeles and Sacramento theories in "neutral territory". It is reassuring that, even though these two theories differ widely in their physical approach, there is no significant difference to be found in their quantitative applications. This is not quite so surprising as it may at first seem since (1) both theories use the same variables, and these variables are the most important in computing rainfall, and (2) both contain empirical coefficients which in effect correct for the errors involved in the basic assumptions.

III

OROGRAPHIC PRECIPITATION THEORY APPLIED TO SMALL BASINS

Basic Model

36. For application to small basins, the Los Angeles orographic-precipitation model, essentially T_{LA1}, has been modified to include the evaluation of effects which should not be neglected when small areas are considered. The basic model is illustrated in figure 2, where

a is the pressure at the nodal surface

b_o is the pressure at the top of the outflow barrier

b_i is the pressure at the top of the inflow barrier

Y is the basin length along the direction of inflow

37. In the Los Angeles Report the statement of mass continuity was approximated by an equation of the form

$$\bar{V}_2 (b_i - a) = \bar{V}_3 (b_o - a) \tag{9}$$

where b_i was taken at sea level or 1000 mb. The expression for rainfall intensity (inches per hour) became

$$I = \frac{\bar{V}_2 W_2 - \bar{V}_3 W_3}{Y} \tag{10}$$

which could be simplified, by substituting for $\bar{V}_3$ from (9), to

$$I = \frac{\bar{V}_2 \left(W_2 - \frac{b_i - a}{b_o - a} W_3 \right)}{Y} \tag{11}$$

38. More exactly (9) and (10) can be expressed as

$$\int_a^{b_i} V_2 \, dp = \int_a^{b_o} V_3 \, dp \tag{12}$$

and

$$I = \frac{\int_{b_i}^{a} V_2 \, dW - \int_{b_o}^{a} V_3 \, dW}{Y} \qquad (13)$$

respectively.

39. The assumptions common to all five equations are:

I. Steady state free from whirls.

II. Current flow everywhere parallel to a definite vertical plane.

III. No frictional effects.

IV. At some upper level (the nodal surface) a horizontal current of constant velocity, above which the atmosphere is undisturbed by orography.

V. A saturated atmosphere with pseudo-adiabatic lapse rate and sea level at 1000 mb.

VI. Loss of mass of air by precipitation of water vapor negligible.

VII. Acceleration of gravity constant.

VIII. All precipitation orographically produced.

IX. Rate of precipitation equal to rate of condensation.

Some of these restrictions will later be removed while otherswill be added, continuing the same system of enumeration. One assumption basic to equations (9), (10), and (11), the assumption that the unweighted mean wind is an adequate approximation, is not contained in (12) and (13).

40. The accuracy of the approximation depends largely upon the vertical shear. If the wind speed does not vary with height, equation (11) is correct. If wind speed increases with height, there is an overestimate of water-vapor transport; if wind speed decreases with height, there is an underestimate. How important quantitatively the vertical shear can be is

[20] illustrated by an analysis of the record San Joaquin storm of January-February 1945.

41. Figure 3 shows three vectors for each rawin observation at Fairfield, Calif., during the storm, Fairfield being representative of inflow at the coast. The solid vectors in the figure represent unweighted mean wind from sea level to 20,000 feet. The dashed vectors represent mean velocity of the same layer weighted by pressure, and the dotted vectors mean velocity weighted by the theoretical moisture content. The direction differences between the vectors for any observation are due to the backing or veering of the wind in the vertical. Since the lowest layers are most heavily weighted with moisture, the moisture-weighted vector most strongly reflects the direction of the wind near the surface. It will therefore fall to the left of the other two vectors when there is a veering with height, and to the right when there is a backing. The upper figure given with each group of vectors expresses as a percentage the ratio of the unweighted mean to the moisture-weighted mean, and the lower figure the ratio of the pressure-weighted to the moisture-weighted mean. The mean ratios in the 1945 storm were 121% in the first case and 116% in the second; raising the nodal surface from 460 to 300 mb would increase the ratios by about 10%.

Wind Shear

42. From hydrostatic relationships defined by the limiting lapse rates and from a consideration of the extreme sea-level density gradients at the peripheries of West Coast storms, a theoretical expression for the vertical gradient of wind speed was developed in the Sacramento Report:

$$V_{1z} = V_{1s} (1 + .06z) \qquad (14)$$

where

V_{1z} is the undisturbed inflow wind at height z

V_{1s} is the frictionless inflow wind at sea level

z is height in thousands of feet above sea level

The equation was presumed to apply up to 10,000 feet.

43. For comparative purposes, the mean relative wind was computed for each level at Fairfield in the 1945 storm by taking the geometric mean of the ratios, for all observations, between the SW component at each level and the SW component at 10,000 feet. A comparison between the values derived from this computation and a similar set of values computed from the Sacramento formula (14) extended to levels above 10,000 feet is shown in figure 4. The results indicate that equation (14) extended to 30,000 feet represents a close fit to the actual shear within a major storm. Henceforth, therefore, the variation of inflow wind with height will be defined by the v_1 curve in figure 5, obtained from a slight modification of (14) in order to smooth the variation with pressure instead of height. The surface wind in this figure is the sea-level frictionless wind in the inflow column (V_{1s}) and the lower-case v will hereinafter denote wind speed as a percentage of V_{1s}.

44. Using subscripts 2 and 3, as in figure 2, for the air columns above the inflow and outflow barriers, respectively, it is now possible, after one other assumption, to derive the wind shear above other points along Y and thus to determine the velocity profile across the basin. Let V_{1p} be the velocity at any pressure in column 1, whose base is at 1000 mb, and V_{2p} the velocity at the same pressure in column 2, whose base is at b_i. The further assumption will be made that

X. The difference between V_{2p} and V_{1p} (or V_{3p} and V_{2p}) is a linear function of pressure, becoming zero at the nodal surface.

Thus

$$V_{2p} - V_{1p} = \alpha (p - a) \tag{15}$$

The equation of continuity, after (12), can then be written

$$\int_a^{1000} V_1 \, dp = \int_a^{b_i} V_1 \, dp + \alpha \int_a^{b_i} (p - a) \, dp$$

whence

$$\alpha = \frac{\int_{b_i}^{1000} V_1 \, dp}{\int_a^{b_i} (p - a) \, dp}$$

Integrating between the designated limits,

$$\alpha = \frac{2\int_{b_i}^{1000} V_1 \, dp}{(b_i - a)^2} \tag{16}$$

Substituting in (15),

$$V_{2p} = V_{1p} + \frac{2\int_{b_i}^{1000} V_1 \, dp}{(b_i - a)^2} (p - a) \tag{17}$$

45. With V_1 defined, the numerator may be integrated between any desired limits and the shear of V_2 determined. The shear of V_3, the velocity above the second or outflow barrier, can be similarly determined from the equation

$$V_{3p} = V_{2p} + \alpha'(p - a)$$

46. Assuming a nodal-surface pressure of 460 mb at the first or inflow barrier and 300 mb at the second or outflow barrier, the mean velocity profile across the basin was computed. In terms of the relative velocity v, the shear in the undisturbed inflow column and in the columns above each of the two barriers is presented in figure 5. Table 6, which

can be entered with b (the pressure at the barrier) and p (any pressure above the barrier), gives the percentages of V_{1s} for various combinations of p and b. Two of the lines in the table, where b equals 896 and 684, give the shears of v_2 and v_3 illustrated in figure 5.

Table 6

VALUES OF v

$(v = 100 \frac{V}{V_{1s}})$

Sfc. Press. b (mb)	Pressure Aloft, p(mb)													
	896	850	800	750	700	684	650	600	550	500	450	400	350	300
896	171	174	178	182	187		192	198	206	214	225	241	256	271
850		200	202	203	206		209	212	218	223	232	246	258	271
800			242	240	238		237	236	238	241	244	254	262	271
750				293	286		278	272	268	263	262	266	268	271
700					357		341	326	312	299	289	283	277	271
684						381	368	349	332	315	300	291	281	271
650							441	411	384	356	332	312	292	271
600								553	502	451	403	359	315	271

Moisture Transport

47. With the wind field defined, the values of the wind may be substituted in the equation for continuity of water vapor (13). Rewritten, using the relative (nondimensional) winds, designated by v, the equation becomes

$$D = \int_{b_i}^{a} v_2 \, dW - \int_{b_o}^{a} v_3 \, dW \qquad (18)$$

D represents the difference, per unit V_{ls}, in equivalent depth of precipitable water transported over the two barriers, after the mean-wind approximation error of (11) has been eliminated.

48. Since a fixed value has been assumed for a, the magnitude of D becomes a function of the two values of b. Integrated over a range of values of b, the relationship between $\int v\, dW$ and b is graphically presented in figure 6. From this figure, D may be determined by taking the difference between ordinates corresponding to the inflow and outflow values of b. In order to convert D to the rainfall intensity I, the relationship

$$I = D \frac{V_{ls}}{Y} \tag{19}$$

must be used.

Spillover

49. The intensity thus obtained is defined as the average rate of precipitation produced by the orographic lift of a basin. It has not been stated whether all of the rain falls into the basin. For an equation such as (13) to express the rate of precipitation in the basin the additional assumption of vertical rainfall must be introduced. This assumption has been made in previous Hydrometeorological Reports, and for large basins the error involved is small. However, because of the hyperbolic effect of Y (the downwind dimension), the shorter this dimension the more serious the error is likely to be. For such basins it is therefore necessary to allow for the fact that, in general, rain does not fall vertically.

50. Define D_{so}, the outflow spillover component, as that portion of D which, though produced by the orographic lift of the basin, falls outside. Similarly, D_{si}, the inflow spillover component, is the portion

of D which falls inside the basin although produced outside. The rate of precipitation within the basin becomes

$$I = \frac{V_{ls}}{Y} (D + D_{si} - D_{so}) \qquad (20)$$

Since D_{so} for an upwind basin is identical with D_{si} for the adjacent downwind basin, it is necessary to solve only for D_{so}. The solution involves, first, an evaluation of the critical raindrop path (i.e., the boundary separating rain which falls inside the basin from rain which falls outside) and, second, the evaluation of the net flow of precipitable water between the boundary and a vertical column above the top of the outflow barrier. The latter computation yields D_{so}.

51. To compute any raindrop path, both the horizontal and vertical velocities of the raindrop are needed. With regard to the first, two extreme possibilities were investigated: (1) at every point the raindrop possesses the horizontal velocity of its environment, and (2) the raindrop starts with the horizontal velocity of its initial environment and maintains the same velocity throughout its path. Within the velocity field described in figure 5, the final results in the two cases do not differ greatly. The first possibility was therefore adopted as assumption XI, because it is more realistic.

52. The horizontal component of the raindrop velocity is thus $v V_{ls}$. On the further assumption (XII) that the slope of the basin in terms of db/dY is constant, the horizontal component of velocity along the raindrop path (ϕ) can be stated:

$$\frac{db_\phi}{dt} = v V_{ls} \frac{(b_o - b_i)}{Y} \qquad (21)$$

where b_i and b_o are the pressures at inflow and at outflow for the particular sub-basins. Combining the basin constants into one,

$$db_\phi = K v \, dt \qquad (22)$$

53. To evaluate the vertical component of the raindrop velocity, the assumption was made that

> XIII. The vertical component equals the algebraic sum of the raindrop's terminal velocity (with respect to still air) and the vertical velocity of the air.

From the data in tables 98 and 99 of the Handbook of Meteorology[7] the mean terminal velocities of raindrops were computed for various intensities of rainfall. It was decided that the data in column 8 of table 98 most nearly characterized the rainfall in the type of storm under consideration and that the appropriate value (neglecting variation with height), computed from these data, was 6.5 mps (assumption XIV). The vertical component due to raindrop terminal velocity thus becomes

$$\frac{dp_\phi}{dt} = 6.5 \frac{\partial p}{\partial z} \tag{23}$$

Combining (22) and (23),

$$db_\phi = \frac{K}{6.5} \frac{v\, dp_\phi}{\partial p/\partial z} \tag{24}$$

With the velocity field already defined as a function of b and p (table 6) and $\partial p/\partial z$ already known from assumption V, it was now possible to integrate (24) by the method of successive approximation. Using K and b_o as parameters, the reverse path of the raindrop was followed from pressure elevations of b_o at 50-mb intervals from 600 to 800 mb and for values of K for intervals of 50 from -50 to -500. Figure 7 shows the results. For comparison, two raindrop paths computed for a constant horizontal velocity (the discarded alternative) are also shown by dashed lines.

54. The effect of the air's vertical velocity on the vertical velocity of the raindrop has still to be considered. A mean evaluation of the effect, based on the following considerations, was used. At the surface the effect is due to ground slope, equal to $\Delta b/\Delta Y$ by assumption XII. At the nodal

surface (300 mb), where by definition the orographic influence ceases, the[27] effect is zero. The raindrop paths computed for figure 7 were therefore adjusted for a mean correction by transposing all points along the path to $p' = p + \Delta b/2$.

55. With the paths determined, the next step in the D_{so} computation was the construction of a streamline chart based on (12). The ordinates p separating equal values of $v \Delta p$ were plotted at each standard b and then connected by smooth curves, as in figure 8. The final curves are thus streamlines and, as reproduced, they bound areas of equal percentages of total mass transport.

56. Computation of D_{so} now resolves itself into an integration of the net flow of precipitable water within each streamline interval and between the critical raindrop path and a vertical at b_o. The final results are shown in figure 9, in terms of the ratio D_{so}/D. Over a wide range of conditions the ratio varies between 10 and 20%. However, it must be remembered that the net spillover is the difference between two such ratios whose denominators may vary considerably.

Upwind Effect

57. Although (20) removes an important restriction, it is still not a complete statement of the rainfall rate for small basins. Both aerodynamic theory and observation indicate that air begins its ascent some distance upwind from the barrier. Qualitatively, the effect is to shift the center of maximum precipitation upwind. Quantitatively, the over-all effect can be estimated empirically.

58. Profiles of the isohyetal patterns of three major storms were drawn along an axis parallel to the inflow wind. The mean values plotted along this axis were chosen from a strip wide enough to qualify the values as representative. Taken along the same strip, the three storm profiles

are shown in figure 10. Four classes of rain are indicated: inflow spillover, upwind rainfall, "orographic" rainfall, and outflow spillover. (For the San Joaquin as a whole, it can be noted, inflow and outflow spillover are approximately equal.) Dividing the volume of rainfall attributable to the upwind effect by the total over the basin produced the following percentages of upwind "loss":

Dec. 9-12, 1937	22.8%
Jan. 19-24, 1943	15.8%
Jan. 30-Feb. 3, 1945	20.7%

The above indicates 20% as fairly representative of the upwind factor U, which can now be used in the rainfall equation

$$I = \frac{V_{ls}}{Y} (1 - U) (D + D_{si} - D_{so}) \qquad (25)$$

Empirical Coefficient

59. In chapter II the maximum possible 66-hour precipitation over the San Joaquin Basin as a whole was determined to be 11.9 inches. The determination was based essentially on a comparison of the geometric properties of the San Joaquin Basin with those of the Sacramento and Los Angeles areas. Now that a general expression for orographic rainfall has been developed on a largely theoretical basis, the 11.9 value may be equated to the theoretical expression in order to derive an empirical coefficient. Because the San Joaquin is so large, equation (19) rather than (25) is applicable, and it can now be written:

$$I = C\, D \frac{V_{ls}}{Y}$$

D can be derived from (18), using 57.5 F as the average 66-hour dewpoint (the mean of the corresponding dewpoints for S_{LA} and S_{SAC}, table 1). The value of Y is available in table 2, and for V_{ls} the mean 66-hour S_{SAC} value, 37.1 mph, was used. The resulting value of the empirical coefficient C is

0.84. (Because the D chart, figure 6, is based upon a 60 F dewpoint, C also contains a dewpoint-correction factor necessary for reduction to 57.5 F. The coefficient for use with a D chart based on 57.5 F would be 0.91.) In the absence of suitable observational data necessary for the determination of the individual coefficients applicable to the sub-basins, it was decided to use the 0.84 coefficient for all basins whose maximum possible precipitation was computed on a purely orographic basis. The computational equation thus becomes

$$I = \frac{C\, V_{1s}}{Y} (1 - U) (D + D_{si} - D_{so}) \qquad (26)$$

Maximum Possible Sub-Basin Orographic Precipitation

60. Equation (26) was considered applicable to the following basins: Calaveras, Stanislaus, Tuolumne, Kings, Kaweah, Tule, and Kern. Because influences other than the orographic character of the sub-basin itself are controlling in each of the five other assigned basins, these basins are dealt with separately in the following chapter.

61. For each sub-basin listed above, inflow and outflow barrier heights were determined by taking mean values for strips one mile wide oriented parallel to the assumed inflow-wind direction. The mean length of all the one-mile strips was taken as Y. The 66-hour precipitation values were computed for inflow from the W, WSW, SW, and S, the optimum direction proving to be SW or WSW for all the basins. The maximum values obtained and the necessary basin constants for their determination are presented in table 7. The Kaweah, Tule, and Calaveras Basins, whose inflow barriers are approximately the height of the Coast Range, receive no inflow spillover since the basins immediately upwind receive only upwind rainfall, from which no outflow can be subtracted. In the Stanislaus and Tuolumne, inflow and outflow spillover are approximately equal. In the Kings, the inflow spillover is approximately one-third the

outflow and in the total Kern and North Fork, the inflow spillover is slightly less than three times the outflow.

Table 7

COMPUTATION OF MAXIMUM 66-HOUR PRECIPITATION OVER OROGRAPHIC SUB-BASINS

Basin	b_i (mb)	b_o (mb)	Y (mi.)	D_{so}	MPP (in.)
Kern, Total	752	677	30.3	11%	15.9
Kern, North Fork	752	677	22.1	15%	21.0
Kern, South Fork	(Total Kern minus North Fork)				10.5
Kings	808	633	31.5	10%	27.6
Tuolumne	807	697	26.6	12%	21.4
Stanislaus	843	689	32.4	10%	23.7
Kaweah	862	684	16.3	17%	45.7
Tule	874	741	16.1	20%	31.9
Calaveras	974	879	23.7	16%	11.9

62. Since S_{SAC} was shown to be the meteorological sequence most appropriate to the San Joaquin, the time distribution in S_{SAC} was considered valid for the basin-wide storm and was also applied to the computed total values of table 7. In percentages of the total value, the time distribution is shown in figure 11. The pertinent maximum depth-duration curves are presented in figures 12-18.

IV

BASINS WITH PRECIPITATION EXCEEDING CALCULATED OROGRAPHIC

Basin Characteristics

63. Rainfall amounts observed over the area embracing five of the assigned sub-basins (Littlejohns, Burns, Bear, Owens, and Mariposa) indicate maximum possible values exceeding those that can be computed from the orographic formula (26). Because these basins all lie either wholly or partly below the elevation of the Coast Range barrier, the Coast Range becomes the effective inflow barrier and differences between outflow and inflow barrier height become negative or, if positive, very small. In addition, because of their size and shape (they are the five smallest of the assigned basins and none of them is particularly elongated), their lengths (Y) are exceptionally short.

64. Despite the small or even negative magnitude of the orographic rainfall over these basins when computed on the basis of the topography within and upwind from the basin itself, the basins are subject to the over-all orographic influences of the San Joaquin and to the special orographic influences of adjoining basins (such as spillover and upwind effects). A fundamental quantitative relationship between the rainfall over these basins and the rainfall over the adjoining basins (particularly downwind) is thus maintained. However, the five basins under consideration are also subject to non-orographic influences such as convergence, frontal and nonfrontal, more effective for short durations, in the maximum case, than the orographic influences. Whereas over such small, low-elevation basins the local intensification of rainfall produced by short-duration non-orographic activity becomes dominant, over the larger, high-

 elevation basins the rain-producing orographic effects overshadow all others, as assumed (VIII) in the development of (26).

Maximum Total Storm

65. The approach to the determination of maximum rainfall values for the five basins under consideration has been empirical, the purpose being to retain relationships between adjoining basins for long durations while including the possibility of the excessive local short-duration activity which is so important for very small basins. Along the optimum inflow-wind direction (WSW) the rainfall profiles of the 1937, 1943, and 1945 storms were drawn across each basin and continued to the eastern edge of the downwind basin for which the maximum possible precipitation had already been computed by (26). From the profile was determined the ratio of the average depth over the lower basin to the average depth over the higher basin. The maximum ratio thus determined was applied to the maximum possible precipitation computed for the higher basin and the result used as the value of the 66-hr maximum possible precipitation over the lower basin. With a greater recorded storm history in the San Joaquin available, these values might be made more reliable, since the maximum ratio from only three major storms was utilized.

Depth-Duration Values

66. Because of the greater importance of localized intensification in these basins, the time distribution of the maximum possible precipitation should differ from the distribution over an area whose rainfall is controlled by orography. A greater percentage of the total precipitation should occur in the shorter durations. To compute this percentage a ratio was established between the maximum observed 24-hr point rainfalls over the lower and higher basins, regardless of concurrence. (All but two of

the maximum 24-hr values occurred in the months November to March, and the two exceptions in September. The storms producing these amounts were all similar in pattern to S_{SAC}.) The theoretical 24-hr maximum precipitation over the higher basin was then multiplied by this ratio to determine the maximum 24-hr precipitation over the lower basin. A 6-hr value was obtained by analysis of the maximum 24-hr precipitation at representative recorder stations (Stockton and Cathay) during the 1943 and 1945 storms. The analysis showed approximately 50% of the maximum 24-hr rainfall occurring in the maximum 6-hr period. Since both storms are prototypes of the San Joaquin maximum possible storm, the same time distribution was applied to the maximum 24-hr precipitation previously derived for the lower basins. To obtain the final depth-duration curves reproduced in figures 19 and 20, smooth curves were drawn through the origin and the values for 6, 24, and 66 hours. A symmetrical distribution through time, similar to figure 11, can be derived from these curves.

67. Burns, Bear, Owens, and Mariposa Creeks have been considered together since they are adjacent and since depth-area differences between them would be a refinement unwarranted by the basic data. The areas of the Burns and Bear Creek drainages assigned are practically the same - 74 and 72 square miles, respectively - and the Mariposa Creek area is 108 square miles. While the small range of area thus involved may be sufficient justification for the lack of individual treatment, a more important justification is the nature of the storm patterns in the region of these basins. In the major storms considered, the isohyets in this region parallel the topographic contours without closing, the closed isohyets occurring farther up slope. This means that basins whose variation in area is due primarily to a variation in width along the same

contours or isohyets will have the same average depth of rainfall regardless of size. The usual decrease of depth with increasing area is characteristic of storm centers and therefore, in the maximum case, of all regions over which the storm can center. However, the usual depth-area relationship need not apply to a region where the basic isohyetal pattern is fixed by topography, specifically to basins like the Burns, Bear, and Mariposa, which are confined between the same isohyets at the edge of the storm pattern.

68. In regions of this kind it may even be possible for a lesser average depth to occur over a smaller adjoining area. The small Owens Creek drainage is a case in point. Its area is only 25.6 square miles but it is confined, in the major storms of record, between isohyets of lesser magnitude than the other three basins because it is, as a whole, farther down slope. On this basis its maximum average rainfall depth may actually be less than over the larger basins. Such a possibility has been neglected for the following reasons. Because its area is one-third to one-fourth the area of the other basins, local intensification could be sufficiently more effective to produce maximum rainfall greater than indicated by the isohyetal gradient. However, no adequate data are available on which to base such a difference. Since the isohyetal-gradient effect and the local-intensification effect are of opposite sign, use of the same depths for the Owens as for the other three basins is considered justifiable.

SNOW MELT

Snow-Melt Factors

69. A theoretical formula, relating rate of snow melt to observations of wind, temperature, and humidity was developed by Light in the Section's Technical Paper No. 1[4/]. Further discussion of its application was contained in chapter VII of the Sacramento Report. The formula is

$$M = k\,U\left[.00184\,(T - 32)\,10^{-.0000156h} + .00578\,(e - 6.11)\right] \qquad (27)$$

where

M is melt in inches of depth of water equivalent per 6-hr period

U is wind speed in mph at the 50-ft level

T is temperature in degrees F at the 10-ft level

e is vapor pressure in mb at the 10-ft level

h is elevation in feet above mean sea level

k is an empirical basin constant for snow-melt runoff

70. Figure 21 is a graphical representation of the formula for computation purposes, with k = 1. Theoretically, k = 1 for melt from a smooth, exposed snow surface. Surface basin characteristics such as rugged topography and forest cover reduce its value below unity. In the present report it is further reduced by the necessary use of free-air wind speeds rather than the unavailable observations at the 50-ft level required by the formula. It was assumed that the ratio of free-air wind to 50-ft wind was a constant but no attempt was made to evaluate the ratio. Instead, it was included in the constant k.

71. Two snow-melt factors not included in (27) are radiation and rainfall. In the maximum storm the net radiational exchange was assumed to be negligible and its effect therefore not computed. However, it was computed for the periods used in the determination of k, the net melting effect of incoming and outgoing radiation being derived from observations of cloudiness and dewpoint. A graphical procedure developed by Wilson[8] was employed, using an albedo of 60% for melting snow.

72. The snow melt due to rainfall can be computed from the formula

$$M = \frac{R\,(T - 32)}{144} \qquad (28)$$

where

M is melt in inches of depth of water equivalent

R is depth of rain in inches

T is temperature of the rain in degrees F, assumed to be the same as that of the air through which it falls.

Figure 22 illustrates the graphical solution of the formula. Melt due to rain was included in the snow melt accompanying the maximum storm but excluded from computations of k because only periods of no rain or negligible rain were selected for analysis in the determination of k.

Determination of Basin Constant

73. The basin constant k is the average ratio of the observed to the theoretical snow melt. It was computed for two basins: the Kings River above Piedra for the 1938, 1941, and 1942 snow-melt seasons, and the Tuolumne River above La Grange for the 1938 snow-melt season.

74. The observed snow-melt runoff was obtained by a summation of the observed discharges for the snow-melt period, corrected for change in reservoir storage in the case of the Tuolumne. No attempt was made to subtract the ground-water base flow. To determine inflow, the observed

discharges were routed by two methods: first, use of channel-storage curves developed by the Langbein[9] procedure from the channel recession of the December 1937 storm; second, use of a routing nomogram developed by Linsley[10]. The channel-storage effect was so small that the observed outflow was used rather than the routed inflow.

75. Although it is preferable that a single station within the basin furnish all the meteorological data for the determination of the theoretical melt, this was not possible in either of the basins. In the Kings River Basin, mean daily temperatures were obtained from Huntington Lake (7000 ft) within the Basin, and all other data from Fresno. In the Tuolumne River Basin, the mean daily temperatures were obtained from Lake Eleanor (4650 ft) within the Basin, wind data from Oakland pibal observations, and all other data from Sacramento. All data were averaged for 5-day periods. Visual inspection of the hydrographs and the index-station mean daily temperatures indicated a 2-day lag between time of melt and arrival of melt water at the gaging station.

76. The snow-line elevation was determined by plotting date of disappearance of the snow on the ground at several stations against station elevation. The resulting snow-line elevation curve for the Tuolumne is shown in figure 23. Melt was assumed to be zero at 32 F, so that the zone of melt became the area between the snow-line elevation and the elevation of the freezing isotherm. The elevation of the freezing isotherm and the temperatures within the zone of melt were obtained by decreasing the average mean daily temperature at the index station by 3.5 F per 1000 ft. For the dewpoint, a lapse rate of 1 F per 1000 ft was used. Wind velocities for the elevations of the zone of melt were obtained from the index-station pibal winds for the corresponding elevations.

77. With the 5-day average mean daily temperature and dewpoint, figure 21 was entered to obtain the melt per 6-hr period, which was multiplied by 20 to obtain the 5-day melt per unit wind velocity. Adjusted for the percentage of basin area covered by the zone of melt (see figure 24, also for the Tuolumne), the 5-day value was then multiplied by the wind velocity to obtain the 5-day snow-melt runoff due to atmospheric turbulence. For the same 5-day period the radiation melt, adjusted for percentage of basin area subject to melt, was also computed. The successive 5-day increments of turbulence and radiation melt were then accumulated for the whole snow-melt season.

78. The values of k for the two basins, determined by dividing the observed snow-melt runoff by the summation of the turbulence and radiation snow-melt runoff, are shown in table 8. Because of lack of unique determinations for other basins in the San Joaquin, the arithmetic average of these values, 0.5, was assumed applicable to all the assigned basins.

Table 8

THEORETICAL AND OBSERVED SNOW MELT (INCHES)
KINGS RIVER ABOVE PIEDRA

Period	Theoretical Melt: Turbulence	Theoretical Melt: Radiation	Theoretical Melt: Total	Observed Runoff	k
Apr. 1-June 29, 1938	25.28	17.58	42.86	21.02	0.49
Apr. 25-June 18, 1941	20.14	11.54	31.68	13.22	0.42
May 1-June 29, 1942	13.62	7.32	20.94	11.71	0.56
TUOLUMNE RIVER ABOVE LA GRANGE (Observed runoff corrected for storage)					
Apr. 1-June 29, 1938	29.95	16.38	46.33	22.2	0.48

79. As a check, the value of k was also computed for the Castle Creek Basin, on the Sierra slopes of the Sacramento Valley, for the 32-day melting

period, April 19-May 20, 1946, during which there was no precipitation. Hourly measurements of temperature, humidity, wind, incident and reflected radiation, and runoff were available, so that even though the Basin does not lie within the San Joaquin, the check is significant. Daily values of snow melt due to atmospheric turbulence were computed from only those hours with temperature above freezing. Donner Summit winds were used as representative of the free-air winds in the Basin. Radiation melt was computed from the corresponding hourly measurements of incident and reflected radiation and an estimate of 13.3 cal/cm^2/hr for the outgoing long-wave radiation[8/]. The observed runoff for the entire period was 25.06 inches. The turbulence melt was computed to be 28.31 inches, and the radiation melt 20.93 inches. The value of k is thus 0.51.

Antecedent Snow Cover

80. A critical rather than a maximum antecedent snow cover will produce the maximum snow-melt contribution accompanying the maximum possible storm. The December 1937 storm is a prime example of a high peak discharge following a light antecedent snow cover. Records show deep snow packs storing both rainfall and snow melt, thus actually reducing peak discharge. Trial routing computations must therefore be made for various antecedent snow covers in order to determine which is critical. Because it is beyond the scope of the assignment to make the necessary trial routings, no definite critical antecedent snow cover is designated in this report. Instead, limits of antecedent snow cover have been designated so that trial routings may be made for values between these limits.

81. A study of the snowfall records in the San Joaquin Valley indicates that the maximum snowstorm of record occurred in January 1933. Snowfall was observed almost every day during the period from the 16th to the 30th. From these data two enveloping curves of snow cover were

derived, the accumulation from the 16th to 19th providing the lower limit and the accumulation from the 16th to 30th the upper limit (figure 25). Because all available snowfall data for the period were used in the determination of these limits, the limits are assumed to apply to all the assigned basins. The snowfall during the maximum possible storm must be added to the assumed antecedent cover but the snow falling during the latter half of the storm is not subject to melting conditions during the period considered. If an antecedent rainstorm is assumed, the antecedent snow cover will have to be reduced by the net melt due to this storm.

Computation of Snow Melt

82. The snow melt accompanying the maximum possible storm was computed for all basins by 1000-ft intervals and 6-hr periods. All steps are shown in a sample computation for the Kings River Basin. Methods and curves used are applicable to all other assigned basins, for which only the final values are given.

83. The meteorological sequence used for the computation, which was adapted from the Sacramento Report, is shown in figure 26. The dewpoint is index to both temperature and humidity, since the air processed in the maximum storm is assumed saturated. Melting conditions were assumed to prevail from 12 hours before the beginning of rain until 12 hours after the end of rain.

84. Since free-air winds were used in the derivation of k, free-air winds should also be used in the snow-melt computation. The variation of the free-air wind velocity with elevation is shown in figure 27, where it is expressed as a percentage of V_{ls}, the frictionless sea-level wind in the undisturbed inflow column. The percentages were determined by comparing the winds at Donner Summit (7200 ft), Blue Canyon (5300 ft), and

Auburn (1600 ft) with the inflow winds at Fairfield during the 1945 storm.[41] To obtain the curve of figure 27, the three percentages were enveloped by a composite theoretical shear taken from table 6 for elevations above the level affected by the Coast Range barrier, and from equation (14) for elevations below that level.

85. The assumed variation of wind with height, the turbulence-melt relationships of figure 21, and the basin constant 0.5 were combined to develop the curves of figure 28 for unit wind velocity. From the curves of figure 28 and the dewpoint sequence of figure 26, values of potential melt from atmospheric turbulence for each 1000-ft elevation zone were determined. These values, per unit wind velocity, are shown in table 9 and apply to all the basins. Multiplied by the appropriate wind velocities, the values are repeated in table 10, also applicable to all basins.

86. Table 11, based on (28) and the assumed variation of temperature during the maximum possible storm (figure 26), gives the incremental potential melt due to rainfall as a percentage of the total-storm average depth, assuming uniform average depth of precipitation at all elevations within one basin. The increments and totals of precipitation, including rainfall and snowfall, are shown in table 12 and the variation of the height of the freezing isotherm during the storm is given in table 13. The percentages shown in table 11 are the same for all basins having the same percentage mass curve of rainfall during the maximum storm. Applied to the total-storm average depth of 27.6 inches over the Kings River Basin, the resulting increments of potential melt due to rainfall are given in table 14. In table 15 the values of tables 10 and 14 are combined to give the increments of total potential snow melt due to both turbulence and rainfall for the Kings River Basin.

87. In table 16 are listed sets of values of depths of antecedent snow cover for each of the basins. For the basins extending above 6000 feet, the depths were selected from figure 25 so that the peak antecedent snow depth at 5000-6000 feet about equaled the total potential melt at that elevation, thus providing for complete melt without storage in the snow pack up to that elevation. For the lower basins, the upper limits of antecedent cover shown in figure 25 were selected. To obtain the total snow depths available for melt, all the values of table 16 must be increased by the snowfall accumulated in the first half of the maximum possible storm. Expressed as percentages of the total-storm precipitation, the increments of snowfall are given in table 17, which is applicable to all basins in which snow falls during the maximum storm. The summations of antecedent and storm snowfall for the Kings River Basin are tabulated in table 18. In table 19 the increments of total potential melt (from table 15) are accumulated until they equal the available snow depth for the zone as shown in table 18. Table 20 shows chronological increments of melt, derived from table 19 for the Kings, and table 21 through 28, derived by similar methods, give the increments for all the other basins. Figure 29 is a graphical summary of the snow melt for the entire storm in the Kings, the average value for each 1000-ft interval being plotted at the midpoint of the interval.

Table 9

INCREMENTS OF POTENTIAL TURBULENCE MELT PER UNIT WIND
ALL BASINS
(Thousandths of an Inch)

Elevation (thousands of feet)	Period Ending (hrs)	-6	0	6	12	18	24	30	36	42	48	54	60	66	72	78
	Reduced Dewpoint (°F)	40	46	51	55	58	61	63	65	63	61	58	55	51	46	40
	0-1	8	16	23	29	34	40	44	48	44	40	34	29	23	16	8
	1-2	4	12	19	25	31	36	40	44	40	36	31	25	19	12	4
	2-3	0	8	15	22	27	33	37	41	37	33	27	22	15	8	0
	3-4	0	4	12	18	24	30	34	38	34	30	24	18	12	4	0
	4-5	0	0	7	14	20	26	30	34	30	26	20	14	7	0	0
	5-6	0	0	3	10	16	22	26	30	26	22	16	10	3	0	0
	6-7	0	0	0	7	13	19	23	28	23	19	13	7	0	0	0
	7-8	0	0	0	3	9	15	20	25	20	15	9	3	0	0	0
	8-9	0	0	0	0	4	11	16	22	16	11	4	0	0	0	0
	9-10	0	0	0	0	0	6	12	17	12	6	0	0	0	0	0
	10-11	0	0	0	0	0	1	7	12	7	1	0	0	0	0	0
	11-12	0	0	0	0	0	0	1	7	1	0	0	0	0	0	0

Table 10

INCREMENTS OF POTENTIAL TURBULENCE MELT ADJUSTED FOR WIND (INCHES)
ALL BASINS

Elevation (thousands of feet)	Period Ending (hrs)	-6	0	6	12	18	24	30	36	42	48	54	60	66	72	78
	Wind Speed (mph)	23	27	30	33	36	38	42	49	42	38	36	33	30	27	23
0-1		0.18	0.43	0.69	0.96	1.22	1.52	1.85	2.35	1.85	1.52	1.22	0.96	0.69	0.43	0.18
1-2		0.09	0.32	0.57	0.82	1.12	1.37	1.68	2.16	1.68	1.37	1.12	0.82	0.57	0.32	0.09
2-3		0	0.22	0.45	0.73	0.97	1.25	1.55	2.01	1.55	1.25	0.97	0.73	0.45	0.22	0
3-4		0	0.11	0.36	0.59	0.86	1.14	1.43	1.86	1.43	1.14	0.86	0.59	0.36	0.11	0
4-5		0	0	0.21	0.46	0.72	0.99	1.26	1.67	1.26	0.99	0.72	0.46	0.21	0	0
5-6		0	0	0.09	0.33	0.58	0.84	1.09	1.47	1.09	0.84	0.58	0.33	0.09	0	0
6-7		0	0	0	0.23	0.47	0.72	0.97	1.37	0.97	0.72	0.47	0.23	0	0	0
7-8		0	0	0	0.10	0.32	0.57	0.84	1.22	0.84	0.57	0.32	0.10	0	0	0
8-9		0	0	0	0	0.14	0.42	0.67	1.08	0.67	0.42	0.14	0	0	0	0
9-10		0	0	0	0	0	0.23	0.50	0.83	0.50	0.23	0	0	0	0	0
10-11		0	0	0	0	0	0.04	0.29	0.59	0.29	0.04	0	0	0	0	0
11-12		0	0	0	0	0	0	0.04	0.34	0.04	0	0	0	0	0	0

Table 11

POTENTIAL SNOW MELT DUE TO RAINFALL
(Hundredths of Percent of Maximum Possible Total-Storm Precipitation)

Elevation (thousands of ft)	Period Ending (hrs) 6	12	18	24	30	36	42	48	54	60	66
MAJOR BASINS *											
0-1	32	99	136	207	290	371	290	207	136	99	32
1-2	27	86	120	185	260	336	260	185	120	86	27
2-3	21	72	104	170	241	313	241	170	104	72	21
3-4	15	59	87	148	212	278	212	148	87	59	15
4-5	8	45	71	126	183	255	183	126	71	45	8
5-6	2	32	60	104	164	220	164	104	60	32	2
6-7	0	18	44	81	135	197	135	81	44	18	0
7-8	0	5	27	67	106	162	106	67	27	5	0
8-9	0	0	11	44	77	128	77	44	11	0	0
9-10	0	0	0	22	58	93	58	22	0	0	0
10-11	0	0	0	0	29	70	29	0	0	0	0
11-12	0	0	0	0	0	35	0	0	0	0	0
LITTLEJOHNS CREEK											
0-1	12	23	61	136	355	889	355	136	61	23	12
1-2	10	20	54	122	318	805	318	122	54	20	10
BURNS, BEAR, OWENS, AND MARIPOSA CREEKS											
0-1	6	23	43	117	376	955	376	117	43	23	6
1-2	5	20	38	104	337	865	337	104	38	20	5
2-3	4	17	33	96	312	806	312	96	33	17	4
3-4	3	14	28	83	275	716	275	83	28	14	3

* Calaveras, Stanislaus, Tuolumne, Kings, Kaweah, Tule, Kern (total), Kern (N.F.), Kern (S.F.)

Table 12. INCREMENTS OF PRECIPITATION DURING MAXIMUM POSSIBLE STORM (INCHES) *

Basin	Period Ending (hrs) 6	12	18	24	30	36	42	48	54	60	66	Total
Calaveras	0.33	0.77	0.93	1.27	1.65	1.99	1.65	1.27	0.93	0.77	0.33	11.9
Stanislaus	0.65	1.54	1.86	2.52	3.29	3.96	3.29	2.52	1.86	1.54	0.65	23.7
Tuolumne	0.59	1.39	1.68	2.28	2.97	3.57	2.97	2.28	1.68	1.39	0.59	21.4
Kings	0.76	1.79	2.17	2.94	3.84	4.61	3.84	2.94	2.17	1.79	0.76	27.6
Kaweah	1.26	2.97	3.59	4.87	6.35	7.63	6.35	4.87	3.59	2.97	1.26	45.7
Tule	0.88	2.07	2.50	3.40	4.43	5.33	4.43	3.40	2.50	2.07	0.88	31.9
Kern (Total)	0.44	1.03	1.25	1.69	2.21	2.66	2.21	1.69	1.25	1.03	0.44	15.9
Kern (N. Fork)	0.58	1.36	1.65	2.24	2.92	3.51	2.92	2.24	1.65	1.36	0.58	21.0
Kern (S. Fork)	0.29	0.68	0.82	1.12	1.46	1.75	1.46	1.12	0.82	0.68	0.29	10.5
Littlejohns	0.06	0.09	0.20	0.40	0.97	2.28	0.97	0.40	0.20	0.09	0.06	5.7
Burns, Bear Owens, Mariposa	0.04	0.12	0.20	0.49	1.46	3.48	1.46	0.49	0.20	0.12	0.04	8.1

Table 13. ELEVATION OF 32 F ISOTHERM - ALL BASINS

Period Ending (hrs)	6	12	18	24	30	36	42	48	54	60	66
Hundreds of Ft	60	76	91	106	120	132	120	106	91	76	60

* Precipitation rainfall below 32 F isotherm, snowfall above.

Table 14

INCREMENTS OF POTENTIAL SNOW MELT DUE TO RAINFALL (INCHES)
KINGS RIVER

Elevation (thousands of ft)	Period Ending (hrs) 6	12	18	24	30	36	42	48	54	60	66
0-1	0.09	0.27	0.38	0.57	0.80	1.02	0.80	0.57	0.38	0.27	0.09
1-2	0.07	0.24	0.33	0.51	0.72	0.93	0.72	0.51	0.33	0.24	0.07
2-3	0.06	0.20	0.29	0.47	0.66	0.86	0.66	0.47	0.29	0.20	0.06
3-4	0.04	0.16	0.24	0.41	0.58	0.77	0.58	0.41	0.24	0.16	0.04
4-5	0.02	0.12	0.20	0.35	0.51	0.70	0.51	0.35	0.20	0.12	0.02
5-6	0.01	0.09	0.17	0.29	0.45	0.61	0.45	0.29	0.17	0.09	0.01
6-7	0	0.05	0.12	0.22	0.37	0.54	0.37	0.22	0.12	0.05	0
7-8	0	0.01	0.07	0.18	0.29	0.45	0.29	0.18	0.07	0.01	0
8-9	0	0	0.03	0.12	0.21	0.35	0.21	0.12	0.03	0	0
9-10	0	0	0	0.06	0.16	0.26	0.16	0.06	0	0	0
10-11	0	0	0	0	0.08	0.19	0.08	0	0	0	0
11-12	0	0	0	0	0	0.10	0	0	0	0	0

Table 15

INCREMENTS OF TOTAL POTENTIAL SNOW MELT (INCHES)
KINGS RIVER

Elevation (thousands of ft)	Period Ending (hrs) -6	0	6	12	18	24	30	36	42	48	54	60	66	72	78
0-1	0.18	0.43	0.78	1.23	1.60	2.09	2.65	3.37	2.65	2.09	1.60	1.23	0.78	0.43	0.18
1-2	0.09	0.32	0.64	1.06	1.45	1.88	2.40	3.09	2.40	1.88	1.45	1.06	0.64	0.32	0.09
2-3	0	0.22	0.51	0.93	1.26	1.72	2.21	2.87	2.21	1.72	1.26	0.93	0.51	0.22	0
3-4	0	0.11	0.40	0.75	1.10	1.55	2.01	2.63	2.01	1.55	1.10	0.75	0.40	0.11	0
4-5	0	0	0.23	0.58	0.92	1.34	1.77	2.37	1.77	1.34	0.92	0.58	0.23	0	0
5-6	0	0	0.10	0.42	0.75	1.13	1.54	2.08	1.54	1.13	0.75	0.42	0.10	0	0
6-7	0	0	0	0.28	0.59	0.94	1.34	1.91	1.34	0.94	0.59	0.28	0	0	0
7-8	0	0	0	0.11	0.39	0.75	1.13	1.67	1.13	0.75	0.39	0.11	0	0	0
8-9	0	0	0	0	0.17	0.54	0.88	1.43	0.88	0.54	0.17	0	0	0	0
9-10	0	0	0	0	0	0.29	0.66	1.09	0.66	0.29	0	0	0	0	0
10-11	0	0	0	0	0	0.04	0.37	0.78	0.37	0.04	0	0	0	0	0
11-12	0	0	0	0	0	0	0.04	0.44	0.04	0	0	0	0	0	0

Table 16

SELECTED ANTECEDENT SNOW COVER
(Inches of Water Equivalent)

Elevation (thousands of ft)	A	B	C
0-1	0.60	0.60	0.90
1-2	1.20	1.30	2.00
2-3	3.10	3.50	6.20
3-4	6.10	6.90	12.20
4-5	9.10	10.40	18.20
5-6	9.90	11.60	22.20
6-7	7.50	8.60	
7-8	5.30	5.80	
8-9	3.80	4.20	
9-10	2.80	3.20	
10-11	2.30	2.60	
11-12	1.90	2.20	
12-13	1.60		

A applies to:	B applies to:	C applies to:
Stanislaus	Kaweah	Calaveras
Tuolumne		Littlejohns
Kings		Burns
Tule		Bear
Kern (Total)		Owens
Kern (N.F.)		Mariposa
Kern (S.F.)		

Table 17

SNOWFALL DEPTH DURING MAXIMUM POSSIBLE STORM *
(Inches of Water Equivalent Expressed as Percent of Total-Storm Precipitation)

Elevation (thousands of ft)	6	12	18	24	30	36	42	48	54	60	66
6-7	2.75	0	0	0	0	0	0	0	0	0	2.75
7-8	2.75	2.60	0	0	0	0	0	0	0	2.60	2.75
8-9	2.75	6.50	0	0	0	0	0	0	0	6.50	2.75
9-10	2.75	6.50	7.06	0	0	0	0	0	7.06	6.50	2.75
10-11	2.75	6.50	7.85	4.26	0	0	0	4.26	7.85	6.50	2.75
11-12	2.75	6.50	7.85	10.65	0	0	0	10.65	7.85	6.50	2.75
12-13	2.75	6.50	7.85	10.65	13.90	0	13.90	10.65	7.85	6.50	2.75

* For Calaveras, Stanislaus, Tuolumne, Kings, Kaweah, Tule, Kern (Total), Kern (N.F.), Kern (S.F.). No snowfall in other basins.

Table 18

SUMMATION OF ANTECEDENT SNOW COVER AND SNOWFALL DURING MAXIMUM POSSIBLE STORM
KINGS RIVER
(Inches of Water Equivalent)

Elevation (thousands of ft)	Period Ending (hrs)													
	-6	0	6	12	18	24	30	36	42	48	54	60	66	72
0-1	0.60	0.60	0.60	0.60	0.60	0.60	0.60	0.60	0.60	0.60	0.60	0.60	0.60	0.60
1-2	1.20	1.20	1.20	1.20	1.20	1.20	1.20	1.20	1.20	1.20	1.20	1.20	1.20	1.20
2-3	3.10	3.10	3.10	3.10	3.10	3.10	3.10	3.10	3.10	3.10	3.10	3.10	3.10	3.10
3-4	6.10	6.10	6.10	6.10	6.10	6.10	6.10	6.10	6.10	6.10	6.10	6.10	6.10	6.10
4-5	9.10	9.10	9.10	9.10	9.10	9.10	9.10	9.10	9.10	9.10	9.10	9.10	9.10	9.10
5-6	9.90	9.90	9.90	9.90	9.90	9.90	9.90	9.90	9.90	9.90	9.90	9.90	9.90	9.90
6-7	7.50	7.50	8.26	8.26	8.26	8.26	8.26	8.26	8.26	8.26	8.26	8.26	9.02	9.02
7-8	5.30	5.30	6.06	6.78	6.78	6.78	6.78	6.78	6.78	6.78	6.78	7.50	8.26	8.26
8-9	3.80	3.80	4.56	6.35	6.35	6.35	6.35	6.35	6.35	6.35	6.35	8.14	8.90	8.90
9-10	2.80	2.80	3.56	5.35	7.30	7.30	7.30	7.30	7.30	7.30	9.25	11.04	11.80	11.80
10-11	2.30	2.30	3.06	4.85	7.02	8.20	8.20	8.20	8.20	9.38	11.55	13.34	14.10	14.10
11-12	1.90	1.90	2.66	4.45	6.62	9.56	9.56	9.56	9.56	12.50	14.67	16.46	17.22	17.22
12-13	1.60	1.60	2.36	4.15	6.32	9.26	13.10	13.10	16.94	19.88	22.05	23.84	24.60	24.60

Table 19

ACCUMULATED SNOW MELT (INCHES)
KINGS RIVER

Elevation (thousands of ft)	Period Ending (hrs) -6	0	6	12	18	24	30	36	42	48	54	60	66	72
0-1	0.18	0.60	0.60	0.60	0.60	0.60	0.60	0.60	0.60	0.60	0.60	0.60	0.60	0.60
1-2	0.09	0.41	1.05	1.20	1.20	1.20	1.20	1.20	1.20	1.20	1.20	1.20	1.20	1.20
2-3	0	0.22	0.73	1.66	2.92	3.10	3.10	3.10	3.10	3.10	3.10	3.10	3.10	3.10
3-4	0	0.11	0.51	1.26	2.36	3.91	5.92	6.10	6.10	6.10	6.10	6.10	6.10	6.10
4-5	0	0	0.23	0.81	1.73	3.07	4.84	7.21	8.98	9.10	9.10	9.10	9.10	9.10
5-6	0	0	0.10	0.52	1.27	2.40	3.94	6.02	7.56	8.69	9.44	9.86	9.90	9.90
6-7	0	0	0	0.28	0.87	1.81	3.15	5.06	6.40	7.34	7.93	8.21	8.21	8.21
7-8	0	0	0	0.11	0.50	1.25	2.38	4.05	5.18	5.93	6.32	6.43	6.43	6.43
8-9	0	0	0	0	0.17	0.71	1.59	3.02	3.90	4.44	4.61	4.61	4.61	4.61
9-10	0	0	0	0	0	0.29	0.95	2.04	2.70	2.99	2.99	2.99	2.99	2.99
10-11	0	0	0	0	0	0.04	0.41	1.19	1.56	1.60	1.60	1.60	1.60	1.60
11-12	0	0	0	0	0	0	0.04	0.48	0.52	0.52	0.52	0.52	0.52	0.52

Table 20

INCREMENTS OF TOTAL SNOW MELT (INCHES)
KINGS RIVER

Elevation (thousands of ft)	Period Ending (hrs) -6	0	6	12	18	24	30	36	42	48	54	60	66	72	Total
0-1	0.2	0.4	0	0	0	0	0	0	0	0	0	0	0	0	0.6
1-2	0.1	0.3	0.6	0.2	0	0	0	0	0	0	0	0	0	0	1.2
2-3	0	0.2	0.5	0.9	1.3	0.2	0	0	0	0	0	0	0	0	3.1
3-4	0	0.1	0.4	0.8	1.1	1.5	2.0	0.2	0	0	0	0	0	0	6.1
4-5	0	0	0.2	0.6	0.9	1.3	1.8	2.4	1.8	0.1	0	0	0	0	9.1
5-6	0	0	0.1	0.4	0.8	1.1	1.5	2.1	1.5	1.1	0.8	0.4	0	0	9.8
6-7	0	0	0	0.3	0.6	0.9	1.3	1.9	1.3	0.9	0.6	0.3	0	0	8.1
7-8	0	0	0	0.1	0.4	0.8	1.1	1.7	1.1	0.8	0.4	0.1	0	0	6.5
8-9	0	0	0	0	0.2	0.5	0.9	1.4	0.9	0.5	0.2	0	0	0	4.6
9-10	0	0	0	0	0	0.3	0.7	1.1	0.7	0.3	0	0	0	0	3.1
10-11	0	0	0	0	0	0	0.4	0.8	0.4	0	0	0	0	0	1.6
11-12	0	0	0	0	0	0	0	0.4	0	0	0	0	0	0	0.4

Table 21

INCREMENTS OF TOTAL SNOW MELT (INCHES)
KAWEAH RIVER

Elevation (thousands of ft)	Period Ending (hrs) -6	0	6	12	18	24	30	36	42	48	54	60	66	72	Total
0-1	0.2	0.4	0	0	0	0	0	0	0	0	0	0	0	0	0.6
1-2	0.1	0.3	0.7	0.2	0	0	0	0	0	0	0	0	0	0	1.3
2-3	0	0.2	0.6	1.1	1.4	0.2	0	0	0	0	0	0	0	0	3.5
3-4	0	0.1	0.4	0.9	1.3	1.8	2.4	0	0	0	0	0	0	0	6.9
4-5	0	0	0.3	0.7	1.0	1.6	2.1	2.8	1.9	0	0	0	0	0	10.4
5-6	0	0	0.1	0.5	0.8	1.3	1.8	2.5	1.8	1.3	0.8	0.5	0	0	11.4
6-7	0	0	0	0.3	0.7	1.1	1.6	2.3	1.6	1.1	0.7	0.3	0	0	9.7
7-8	0	0	0	0.1	0.4	0.9	1.3	2.0	1.3	0.9	0.4	0.1	0	0	7.4
8-9	0	0	0	0	0.2	0.6	1.0	1.7	1.0	0.6	0.2	0	0	0	5.3
9-10	0	0	0	0	0	0.3	0.8	1.2	0.8	0.3	0	0	0	0	3.4
10-11	0	0	0	0	0	0	0.4	0.9	0.4	0	0	0	0	0	1.7
11-12	0	0	0	0	0	0	0.2	0.7	0.2	0	0	0	0	0	1.1

Table 22

INCREMENTS OF TOTAL SNOW MELT (INCHES)
STANISLAUS RIVER

Elevation (thousands of ft)	Period Ending (hrs) -6	0	6	12	18	24	30	36	42	48	54	60	66	72	Total
0-1	0.2	0.4	0	0	0	0	0	0	0	0	0	0	0	0	0.6
1-2	0.1	0.3	0.6	0.2	0	0	0	0	0	0	0	0	0	0	1.2
2-3	0	0.2	0.5	0.9	1.2	0.3	0	0	0	0	0	0	0	0	3.1
3-4	0	0.1	0.4	0.7	1.1	1.5	1.9	0.4	0	0	0	0	0	0	6.1
4-5	0	0	0.2	0.6	0.9	1.3	1.7	2.2	1.7	0.5	0	0	0	0	9.1
5-6	0	0	0.1	0.4	0.7	1.1	1.5	2.0	1.5	1.1	0.7	0.4	0.1	0	9.6
6-7	0	0	0	0.3	0.6	0.9	1.3	1.8	1.3	0.9	0.6	0.3	0	0	8.0
7-8	0	0	0	0.1	0.4	0.7	1.1	1.6	1.1	0.7	0.4	0.1	0	0	6.2
8-9	0	0	0	0	0.2	0.5	0.8	1.4	0.8	0.5	0.2	0	0	0	4.4
9-10	0	0	0	0	0	0.3	0.6	1.0	0.6	0.3	0	0	0	0	2.8
10-11	0	0	0	0	0	0	0.4	0.8	0.4	0	0	0	0	0	1.6

Table 23

INCREMENTS OF TOTAL SNOW MELT (INCHES)
TUOLUMNE RIVER

Elevation (thousands of ft)	Period Ending (hrs) -6	0	6	12	18	24	30	36	42	48	54	60	66	72	Total
0-1	0.2	0.4	0	0	0	0	0	0	0	0	0	0	0	0	0.6
1-2	0.1	0.3	0.6	0.2	0	0	0	0	0	0	0	0	0	0	1.2
2-3	0	0.2	0.5	0.9	1.2	0.3	0	0	0	0	0	0	0	0	3.1
3-4	0	0.1	0.4	0.7	1.0	1.5	1.9	0.5	0	0	0	0	0	0	6.1
4-5	0	0	0.2	0.6	0.9	1.3	1.6	2.2	1.6	0.7	0	0	0	0	9.1
5-6	0	0	0.1	0.4	0.7	1.1	1.4	1.9	1.4	1.1	0.7	0.4	0.1	0	9.3
6-7	0	0	0	0.3	0.6	0.9	1.3	1.8	1.3	0.9	0.6	0.3	0	0	8.0
7-8	0	0	0	0.1	0.4	0.7	1.1	1.6	1.1	0.7	0.4	0.1	0	0	6.2
8-9	0	0	0	0	0.2	0.5	0.8	1.4	0.8	0.5	0.2	0	0	0	4.4
9-10	0	0	0	0	0	0.3	0.6	1.0	0.6	0.3	0	0	0	0	2.8
10-11	0	0	0	0	0	0	0.4	0.7	0.4	0	0	0	0	0	1.5
11-12	0	0	0	0	0	0	0	0.4	0	0	0	0	0	0	0.4

Table 24

INCREMENTS OF TOTAL SNOW MELT (INCHES)
TULE RIVER

Elevation (thousands of ft)	Period Ending (hrs) -6	0	6	12	18	24	30	36	42	48	54	60	66	72	Total
0-1	0.2	0.4	0	0	0	0	0	0	0	0	0	0	0	0	0.6
1-2	0.1	0.3	0.7	0.1	0	0	0	0	0	0	0	0	0	0	1.2
2-3	0	0.2	0.5	1.0	1.3	0.1	0	0	0	0	0	0	0	0	3.1
3-4	0	0.1	0.4	0.8	1.1	1.6	2.1	0	0	0	0	0	0	0	6.1
4-5	0	0	0.2	0.6	1.0	1.4	1.8	2.5	1.6	0	0	0	0	0	9.1
5-6	0	0	0.1	0.4	0.8	1.2	1.6	2.1	1.6	1.2	0.8	0.1	0	0	9.9
6-7	0	0	0	0.3	0.6	1.0	1.4	2.0	1.4	1.0	0.6	0.1	0	0	8.4
7-8	0	0	0	0.1	0.4	0.8	1.2	1.7	1.2	0.8	0.4	0.1	0	0	6.7
8-9	0	0	0	0	0.2	0.6	0.9	1.5	0.9	0.6	0.2	0	0	0	4.9
9-10	0	0	0	0	0	0.3	0.7	1.1	0.7	0.3	0	0	0	0	3.1

Table 25

INCREMENTS OF TOTAL SNOW MELT (INCHES)
KERN RIVER, TOTAL BASIN

Elevation (thousands of ft)	Period Ending (hrs) -6	0	6	12	18	24	30	36	42	48	54	60	66	72	Total
2-3	0	0.2	0.5	0.8	1.2	0.4	0	0	0	0	0	0	0	0	3.1
3-4	0	0.1	0.4	0.7	1.0	1.4	1.7	0.8	0	0	0	0	0	0	6.1
4-5	0	0	0.2	0.5	0.8	1.2	1.6	2.1	1.6	1.1	0	0	0	0	9.1
5-6	0	0	0.1	0.4	0.7	1.0	1.4	1.8	1.4	1.0	0.7	0.4	0.1	0	9.0
6-7	0	0	0	0.3	0.5	0.8	1.2	1.7	1.2	0.8	0.5	0.3	0	0	7.3
7-8	0	0	0	0.1	0.4	0.7	1.0	1.5	1.0	0.7	0.4	0.1	0	0	5.9
8-9	0	0	0	0	0.2	0.5	0.8	1.3	0.8	0.5	0.2	0	0	0	4.3
9-10	0	0	0	0	0	0.3	0.6	1.0	0.6	0.3	0	0	0	0	2.8
10-11	0	0	0	0	0	0	0.3	0.7	0.3	0	0	0	0	0	1.3
11-12	0	0	0	0	0	0	0	0.4	0	0	0	0	0	0	0.4

Table 26

INCREMENTS OF TOTAL SNOW MELT (INCHES)
KERN RIVER, NORTH FORK

Elevation (thousands of ft)	Period Ending (hrs) -6	0	6	12	18	24	30	36	42	48	54	60	66	72	Total
2-3	0	0.2	0.5	0.9	1.2	0.3	0	0	0	0	0	0	0	0	3.1
3-4	0	0.1	0.4	0.7	1.0	1.5	1.9	0.5	0	0	0	0	0	0	6.1
4-5	0	0	0.2	0.6	0.9	1.3	1.6	2.2	1.6	0.7	0	0	0	0	9.1
5-6	0	0	0.1	0.4	0.7	1.1	1.4	1.9	1.4	1.1	0.7	0.4	0.1	0	9.3
6-7	0	0	0	0.3	0.6	0.9	1.2	1.8	1.2	0.9	0.6	0.3	0	0	7.8
7-8	0	0	0	0.1	0.4	0.7	1.1	1.6	1.1	0.7	0.4	0.1	0	0	6.2
8-9	0	0	0	0	0.2	0.5	0.8	1.4	0.8	0.5	0.2	0	0	0	4.4
9-10	0	0	0	0	0	0.3	0.6	1.0	0.6	0.3	0	0	0	0	2.8
10-11	0	0	0	0	0	0	0.4	0.7	0.4	0	0	0	0	0	1.5
11-12	0	0	0	0	0	0	0	0.4	0	0	0	0	0	0	0.4

Table 27

INCREMENTS OF TOTAL SNOW MELT (INCHES)
KERN RIVER, SOUTH FORK

Elevation (thousands of ft)	Period Ending (hrs) -6	0	6	12	18	24	30	36	42	48	54	60	66	72	Total
2-3	0	0.2	0.5	0.8	1.1	0.5	0	0	0	0	0	0	0	0	3.1
3-4	0	0.1	0.4	0.6	1.0	1.3	1.6	1.1	0	0	0	0	0	0	6.1
4-5	0	0	0.2	0.5	0.8	1.1	1.5	1.9	1.5	1.1	0.5	0	0	0	9.1
5-6	0	0	0.1	0.4	0.6	0.9	1.3	1.7	1.3	0.9	0.6	0.4	0.1	0	8.3
6-7	0	0	0	0.3	0.5	0.8	1.1	1.6	1.1	0.8	0.5	0.3	0	0	7.0
7-8	0	0	0	0.1	0.4	0.6	1.0	1.4	1.0	0.6	0.4	0.1	0	0	5.6
8-9	0	0	0	0	0.2	0.5	0.7	1.2	0.7	0.5	0.2	0	0	0	4.0
9-10	0	0	0	0	0	0.2	0.6	0.9	0.6	0.2	0	0	0	0	2.5
10-11	0	0	0	0	0	0	0.3	0.7	0.3	0	0	0	0	0	1.3
11-12	0	0	0	0	0	0	0	0.4	0	0	0	0	0	0	0.4

Table 28

INCREMENTS OF TOTAL SNOW MELT (INCHES)

Elevation (thousands of ft)	Period Ending (hrs) -6	0	6	12	18	24	30	36	42	48	54	60	66	72	Total
CALAVERAS RIVER															
0-1	0.2	0.4	0.3	0	0	0	0	0	0	0	0	0	0	0	0.9
1-2	0.1	0.3	0.6	0.9	0.1	0	0	0	0	0	0	0	0	0	2.0
2-3	0	0.2	0.5	0.8	1.1	1.5	1.8	0.3	0	0	0	0	0	0	6.2
3-4	0	0.1	0.4	0.7	0.9	1.3	1.7	2.2	1.7	1.3	0.9	0.7	0.3	0	12.2
4-5	0	0	0.2	0.5	0.8	1.1	1.5	2.0	1.5	1.1	0.8	0.5	0.2	0	10.2
5-6	0	0	0.1	0.4	0.6	1.0	1.3	1.7	1.3	1.0	0.6	0.4	0.1	0	8.5
LITTLEJOHNS CREEK															
0-1	0.2	0.4	0.3	0	0	0	0	0	0	0	0	0	0	0	0.9
1-2	0.1	0.3	0.6	0.8	0.2	0	0	0	0	0	0	0	0	0	2.0
BURNS, BEAR, OWENS, AND MARIPOSA CREEKS															
0-1	0.2	0.4	0.3	0	0	0	0	0	0	0	0	0	0	0	0.9
1-2	0.1	0.3	0.6	0.8	0.2	0	0	0	0	0	0	0	0	0	2.0
2-3	0	0.2	0.5	0.7	1.0	1.3	1.8	0.7	0	0	0	0	0	0	6.2
3-4	0	0.1	0.4	0.6	0.9	1.2	1.7	2.4	1.7	1.2	0.9	0.6	0.4	0.1	12.2

VI

TESTS AND ADAPTATIONS

Test of Orographic Formula

88. An appropriate test of the orographic-rainfall formula (26) developed in chapter III would be to use it in computing the rainfall values in the major storms from measurements of topographic and meteorological parameters and to compare these computed values with the observed rainfall. Good comparisons from a number of major storms would verify the formula. However, such comparisons are reduced in accuracy by the inadequacies of both types of data used. Not only are the meteorological observations of wind and moisture content (particularly from the point of view of representativeness) sometimes of doubtful character, but the so-called "observed rainfall" is really a computed value which may be largely based on interpolations between observations too sparse to be areally reliable. In some basins there are actually no rainfall stations or stream gages. The comparisons are therefore qualitative rather than quantitative.

89. In the San Joaquin Basin there is available only one storm (January-February 1945) with sufficient meteorological data to permit a comparison of calculated and observed rainfall. Even in this storm the necessary extrapolations and interpolations from the observed data make the comparison qualitative rather than quantitative. For each rawin observation at Fairfield a mean 10,000-ft WSW component of the wind was determined and reduced to sea level (V_{ls}) in accordance with the assumed wind shear in the theoretical development. A correction factor was applied to moisture content in order to compensate for the

deviation of representative storm dewpoints from the assumed dewpoints of the critical storm sequence of figure 26. No adjustments were made for lag between observed wind and dewpoint and observed precipitation.

90. The accumulated calculated 6-hr increments of rainfall are plotted against the observed for the same duration in figure 30. Of the nine basins for which the comparison was made, five show a good agreement between calculated and observed precipitation. A number of analyses were made to relate the magnitude of the discrepancies to topographic or meteorological parameters. The best of these relations is shown in figure 31, where the average inflow-barrier height of each basin is plotted against the difference between calculated and observed precipitation. Excluding the Calaveras, which is not affected by the Coast Range, the figure shows the difference to be the greatest for the basins whose average inflow barriers are about the height of the Coast Range barrier. A depleting effect of the Coast Range is thus indicated beyond that which was included in the development of the theoretical equation. Should future storms support this indication, an empirical correction factor could be approximated, but the data from a single storm are not sufficient basis for its introduction at this time. Moreover, the 1945 storm did not have maximum wind velocities, and it is possible that the indicated depleting effect of the Coast Range might be less pronounced under maximum-wind conditions.

Test of Snow-Melt Formula

91. The formula (27) used to compute the snow melt due to turbulence implies a melting rate directly proportional to wind speed. There is some reason to believe that the relationship may not be linear, that the wind-speed factor should have an exponent less than unity. Several investigations, aimed at the modification of the wind factor, were conducted.

92. One investigation was based on nine years of data from Wagon Wheel Gap, Colo. The available data were precipitation amount, character of precipitation, snow depth on ground, density of snow on ground, wind movement, and hourly temperature. The data were summarized for periods varying from five to seven days and the number of degree days and average wind speed computed for each period. The accompanying snow melt, confined by the data to the point of observation, was computed from observations of the initial and final water equivalent of the snow on the ground and the intervening snowfall. Periods with both snowfall and rainfall were excluded because separation of the amounts was not possible. Some periods actually showed an increase of water equivalent of snow depth exceeding the snowfall during the period. Such periods, excluded as inaccurate, illustrate the difficulties of measurement and calculation of snow melt at a point. In addition to inaccuracies of measurement, important sources of error are the drifting of snow and the storage of water in snow. Even the periods selected for analysis included errors from some of these sources.

93. In order to study the effect of wind speed alone on the rate of snow melt, the average amount of melt per degree day was calculated for each value of wind speed from four to ten miles per hour. Although showing an irregular fluctuation, these amounts indicated an increase of snow melt with increasing wind speed. From so small a range of wind speeds, however, it was not possible to determine whether the relationship was linear or non-linear. There were only six cases of average wind speed over 10 mph and none over 13 mph. Unfortunately, the data did not permit melt computations for periods short enough to be accompanied by higher average wind speeds.

94. An attempt was made to relate snow melt to the intensity of storm rainfall and thus to bypass the necessity for using a relationship

of snow melt to wind speed. Such a procedure involves the assumption that the variations of wind speed, temperature, and humidity would all be reflected in the rainfall intensity. Again the analysis was confined to the evidences of snow melt at one observation station - Lake Eleanor (4650 ft), in the Tuolumne River Basin. A 30-year daily record of precipitation amount, character of precipitation, snowfall, and depth of snow on ground was scanned for occurrences of excessive rainfall on an antecedent snow cover. Seven good cases were found. A snow density of 0.28 was assumed to apply to the decrease of depth of snow on the ground. The resulting plot of snow melt against rainfall depth during the calendar 24-hr periods of heaviest rainfall showed a fairly good linear relationship. Extrapolation to the maximum possible storm gave a snow-melt value for the maximum 24-hr period of the storm less than half the theoretically computed value for the interval from 4000 to 5000 feet in the Tuolumne Basin (figure 19).

95. In both the above investigations, unavailability of adequate and synchronized data was a serious deficiency. The hourly records of the Central Sierra Snow Laboratory (Castle Creek Basin), although the period of record is still too short, constitute the best available data. In a further investigation, these data were subjected to a series of statistical tests to determine the element or combination of elements which would serve as the best index to the rate of snow melt. Daily values of temperature, dewpoint, wet-bulb temperature, vapor pressure, wind speed, radiation, and combinations of these elements were correlated with runoff for the 32-day period without precipitation which was used in chapter V for a check determination of k.

96. Of the indices tested, the wet-bulb temperature, expressed as the sum of degree hours divided by 24, was the best single daily index.

A combined index, using the temperature and the vapor-pressure difference between air and snow surface was almost as reliable. Both were better indices than temperature alone, i.e., the simple degree-day factor.

97. The incorporation of wind speed or radiation as a factor did not improve the correlation. This was not taken to mean that these elements are insignificant, but that the period of record was too short to evaluate their effect. For example, the highest daily wind speed reached during the period was only nine miles per hour. This was too low a value from which to extrapolate to the extremely high winds of the maximum possible storm. The use of the stronger winds at Donner Summit during the 32-day period did not improve the results.

98. Since the data would not yield an empirical formula which could be considered reliable, and since the effect of wind speed and radiation could not be evaluated, it was decided to retain the theoretical formula now used. This can be justified as follows: The data show that temperature and vapor pressure are a good index to the rate of snow melt, and these elements are used in the formula. Also, the use of Donner Summit winds in the formula verified the value of k as 0.5. Since the formula gives the melting rate due to atmospheric turbulence only, it can be applied to the maximum possible storm in which radiation is assumed to be negligible.

Distribution of Precipitation

99. A particular time distribution of the maximum possible precipitation has been used in the chapter on snow melt. It is the distribution consistent with the symmetrical wind and dewpoint sequence of figure 26 and with the general patterns of the mass curves of precipitation in the 1937, 1943, and 1945 major storms previously cited. However, since there is no adequate basis for the determination of a rigidly defined sequence

of winds and dewpoints or the sequence of the resulting precipitation, 12-hr changes from the suggested pattern of precipitation periods (table 12) are permissible for hydrologic trial. Any such rearrangement implies the same rearrangement of the wind and dewpoint sequences and of the progressive elevation of the freezing isotherm. Therefore, the increments of total potential snow melt (table 15) and of the snowfall depth (table 17) would have to be similarly rearranged. As a final result, the increments of total snow melt (tables 20-28) may change in magnitude as well as in chronological position.

100. Since the pattern of areal distribution of the maximum storm within each basin is not known, this report recommends no particular distribution with area within each sub-basin nor even a variation of the maximum precipitation with altitude within the sub-basin. Despite the indications of a distribution of precipitation with altitude suggested in figure 31 and in the discussion (chapter IV) justifying the combination of small, low-level basins in figure 20, the Section has not felt justified in accepting any indicated pattern as necessarily valid in the case of the maximum possible storm. The assumptions basic to both the theoretical and empirical computations do not warrant extension of the computation methods beyond the calculation of the undistributed average depth.

101. Any consistent pattern of precipitation variation with height, such as shown by mean seasonal isohyets, is the product of more factors than elevation, slope, aspect, and the other parameters specific to the topography. Storm-type frequency and prevailing air-mass characteristics are other very important factors. The average storm whose recurrence produces the mean seasonal pattern, is not characterized by the wind speed and constancy of direction postulated for the maximum possible storm, nor

is the average inflowing air mass saturated at all levels as in the maximum storm. It is apparent, for instance, that the higher the condensation level within the inflowing air mass, the higher up slope will be the zone of most intense precipitation. In the air mass processed for the maximum storm, the condensation level is sea level. In the ordinary air mass, the lowest layers (the layers of maximum moisture content in the maximum storm) do not even become saturated until they have moved some distance up slope. In the maximum storm they are saturated before any lift begins. For these reasons, redistribution of precipitation with height according to a pattern developed from ordinary storms cannot be recommended. It is not inconceivable that the variation with height may even be reversed in the maximum possible storm. The patterns of variation shown by the major storms, although they offer a better clue, may be doubted for similar reasons.

102. Should any variation from the uniform distribution of precipitation be introduced for hydrologic trial, two important restrictions must be observed. One is that the redistribution should leave the maximum possible depth of precipitation over the particular basin unchanged. The other restriction is that the values of snowfall and of snow melt due to rainfall (tables 11, 14, and 17) for each elevation interval should be changed proportionately and the total snow melt recalculated. For some redistributions, such changes in snowfall and snow melt would in turn necessitate a change in the assumed antecedent snow cover.

103. Redistribution, in time or in space, within any basin and for evaluation of the discharge at the dam site for the specific basin, may be accomplished without consideration of other basins. The report does not imply that the maximum possible precipitation over all of the basins will occur within the same storm.

104. Recalculation of snow cover as well as of snow melt will be required if, for hydrologic trial, the occurrence of another rainstorm is assumed as antecedent to the maximum possible storm. Snow-melt computations applied to the January-February 1945 storm, for instance, indicate that below 4000 feet the optimum snow cover would be entirely melted. In addition, certain minimum intervals of storm recurrence (here defined as the period between the peaks of antecedent and maximum possible precipitation) should be observed in timing the antecedent storm. While any historical storm may be used as the antecedent storm, the minimum recurrence interval for the major storms of March 1937, January 1943, and January-February 1945, should be no less than seven days; for all other known storms in the region the minimum interval may be kept at four days.

REFERENCES

1. HMS, Off. Hyd. Dir., USWB, Maximum possible precipitation over the Sacramento Basin of California, Hydrometeorological Report No. 3, 1943, in coop. with Corps of Engineers, War Dept.

2. HMS, Off. Hyd. Dir., USWB, Revised report on maximum possible precipitation, Los Angeles area, California, Hydrometeorological Report No. 21B, 1945, in coop. with Corps of Engineers, War Dept.

3. F. Pockels, The theory of the formation of precipitation on mountain slopes, MWR, v. 29, Apr. 1901, p. 152-9; also in Mechanics of the earth's atmosphere, ed. by C. Abbe, 1910, p. 80-104. (Translation from Annalen der Physik, ser. 4, v. 4, no. 3, p. 459-80, 1901.)

4. P. Light, Analysis of high rates of snow melting, Hydrometeorological Section Technical Paper No. 1, in Appendix to Hydrometeorological Report No. 2, Maximum possible precipitation over the Ohio River Basin above Pittsburgh, Pennsylvania, HMS, Off. Hyd. Dir., USWB, 1941. Also, TAGU, 1941, pt. 1, p. 195-205.

5. T. R. Reed, Weather types of the northeast Pacific Ocean as related to weather of the North Pacific Coast, MWR, v. 60, Dec. 1932, p. 246-52.

6. J. A. Brown, Weather map types for use in daily forecasting of winter rainfall amounts at Los Angeles, California, USWB, 1943.

7. F. A. Berry, E. Bollay, and N. R. Beers, Handbook of meteorology, sec. 1, Numerical and graphical data, p. 114-15, tables 98-9.

8. W. T. Wilson, An outline of the thermodynamics of snow melt, TAGU, 1941, pt. 1, p. 182-95.

9. W. B. Langbein, Some channel storage studies and their applications to the determination of infiltration, TAGU, 1938, pt. 1, p. 435-47.

10. R. K. Linsley, Fresno River District Technical Report No. 1, USWB, 1943.

Abbreviations

HMS - Hydrometeorological Section, Division of Climatological and Hydrologic Services (formerly Office of Hydrologic Director), U. S. Weather Bureau.

MWR - Monthly Weather Review, U.S. Weather Bureau

Off. Hyd. Dir. - Office of Hydrologic Director (after July 1946, Division of Climatological and Hydrologic Services), U.S. Weather Bureau

TAGU - Transactions of the American Geophysical Union

USWB - U.S. Weather Bureau

SCHEMATIC OROGRAPHIC MODELS

Adapted from Los Angeles Report

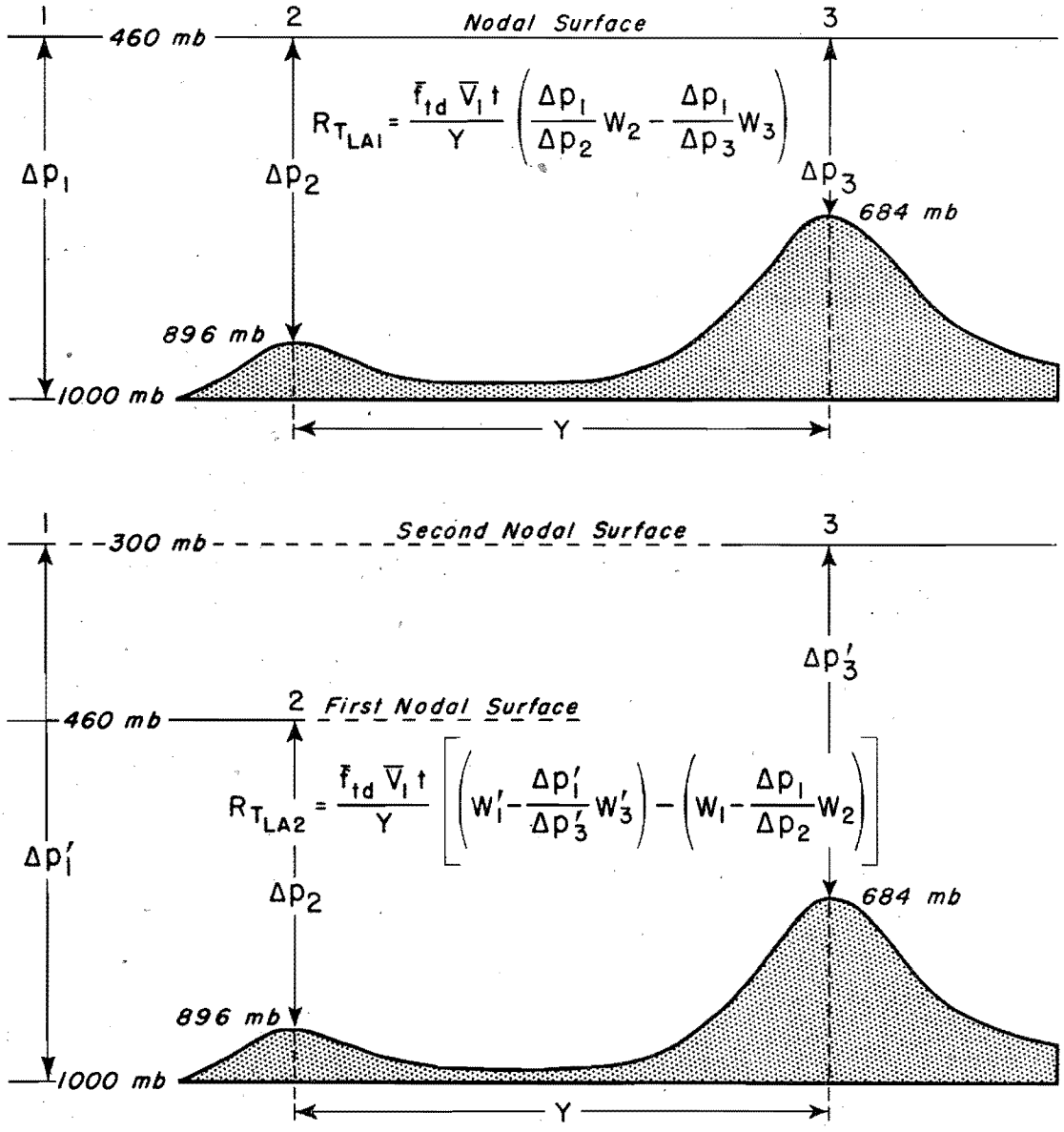

SCHEMATIC OROGRAPHIC MODEL FOR SUB-BASIN COMPUTATION

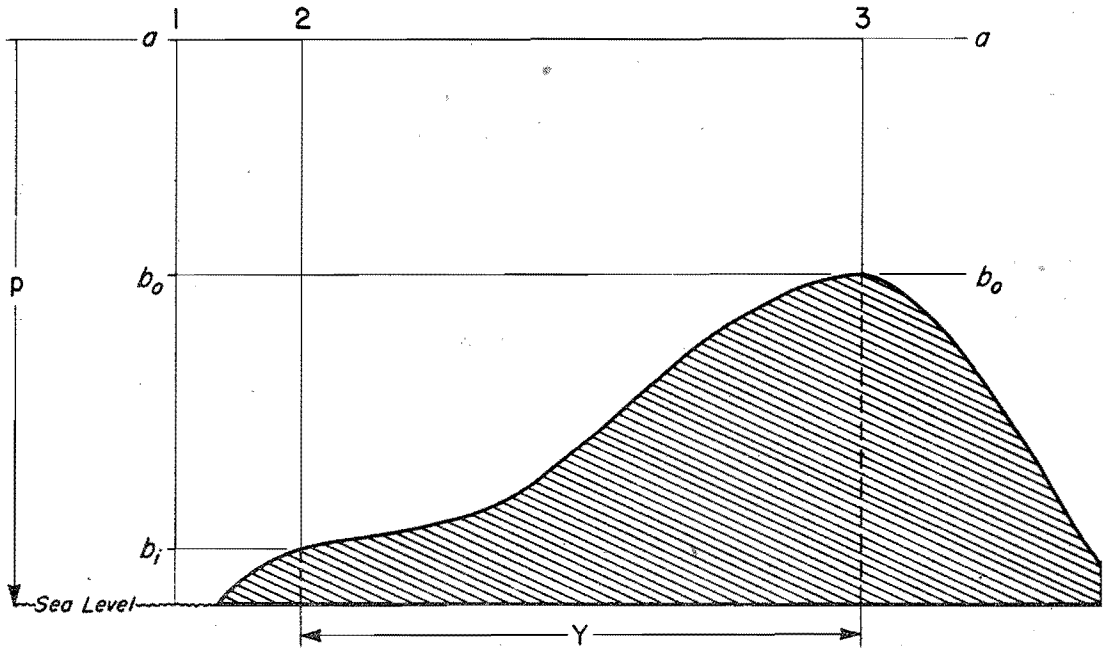

File 47002 Hydrometeorological Report 24 Figure 2

WINDS AT FAIRFIELD, CALIFORNIA
Mean of Layer, Surface to 20000 Feet

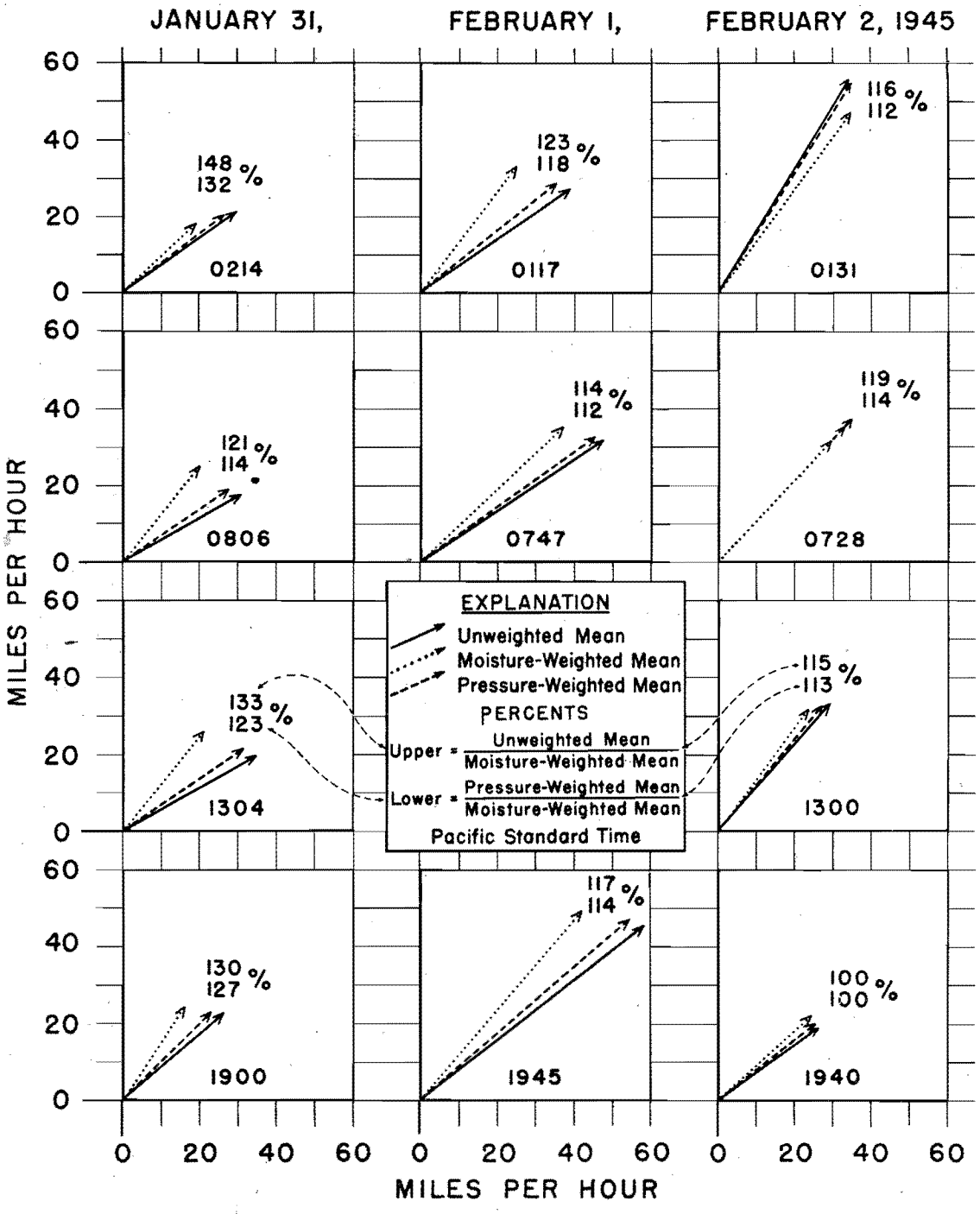

File 47002 Hydrometeorological Report 24 Figure 3

MEAN SHEAR OF INFLOW WINDS
Sacramento and San Joaquin River Basins

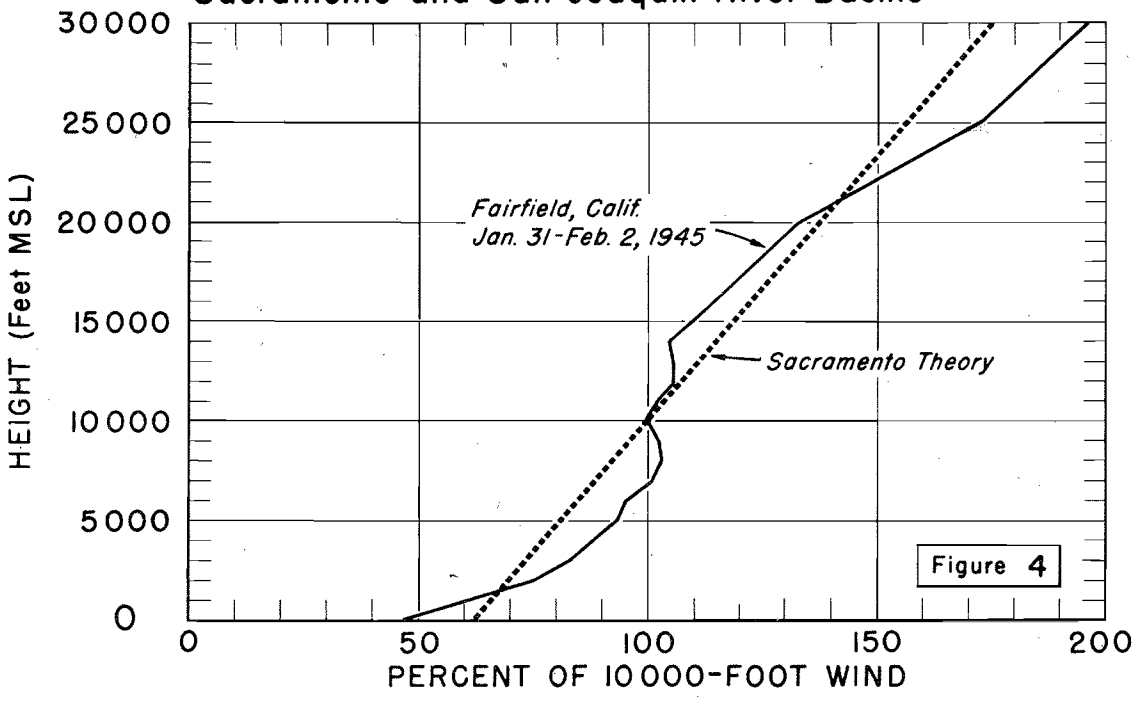

THEORETICAL WIND PROFILE
San Joaquin River Basin Maximum Storm

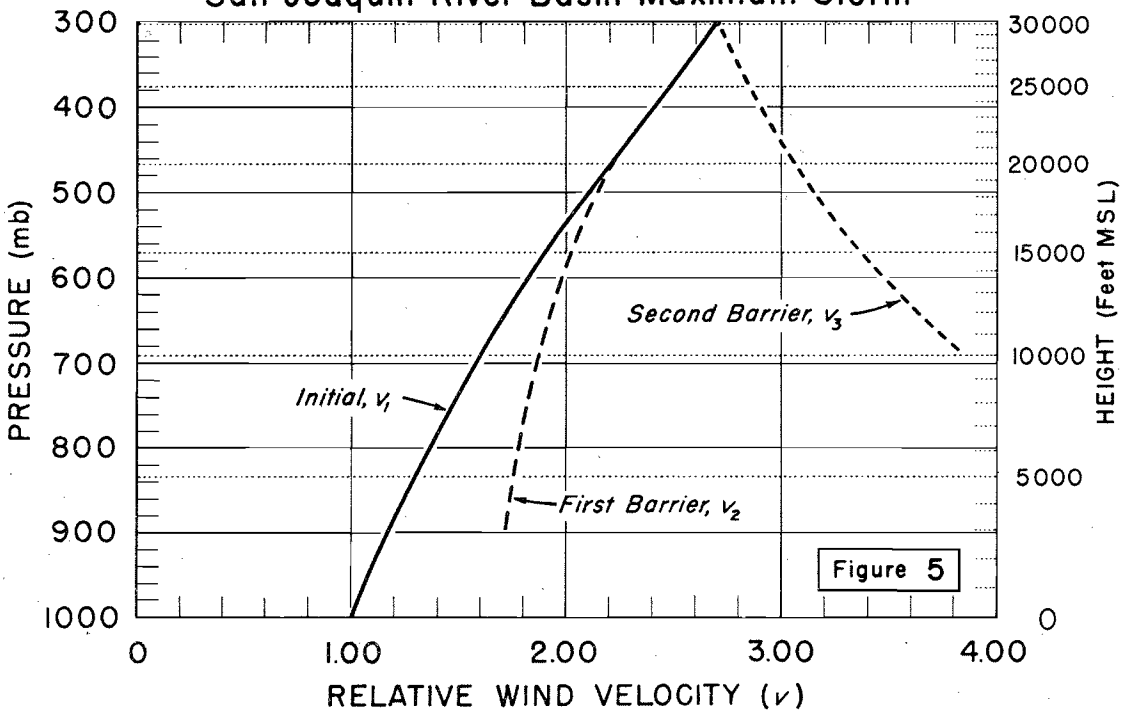

D COMPUTATION CHART
San Joaquin River Basin Maximum Storm

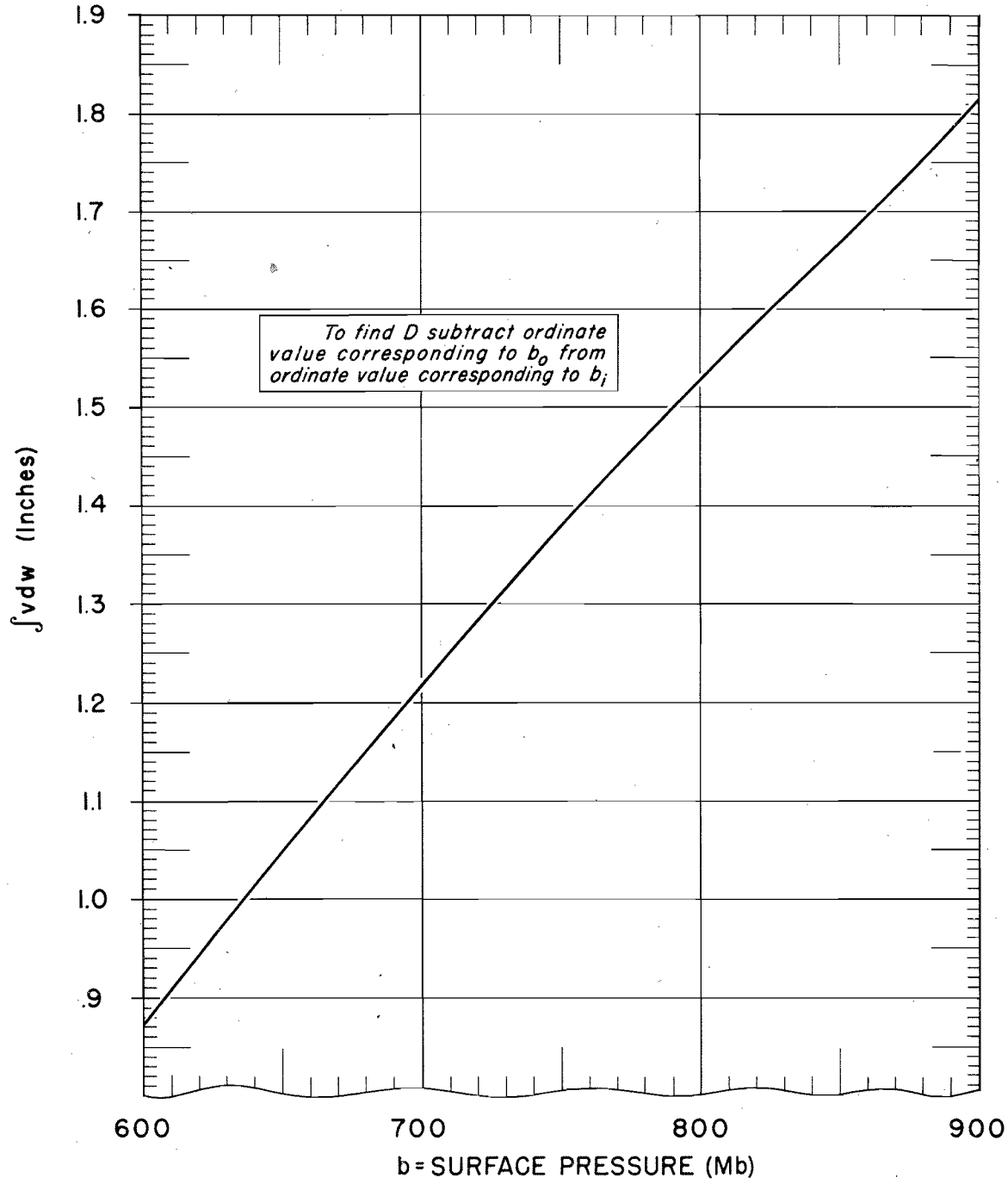

File 47002 Hydrometeorological Report 24 Figure **6**

COMPUTED RAINDROP PATHS

San Joaquin River Basin Maximum Storm

——— = Assumption 1

- - - - = Assumption 2

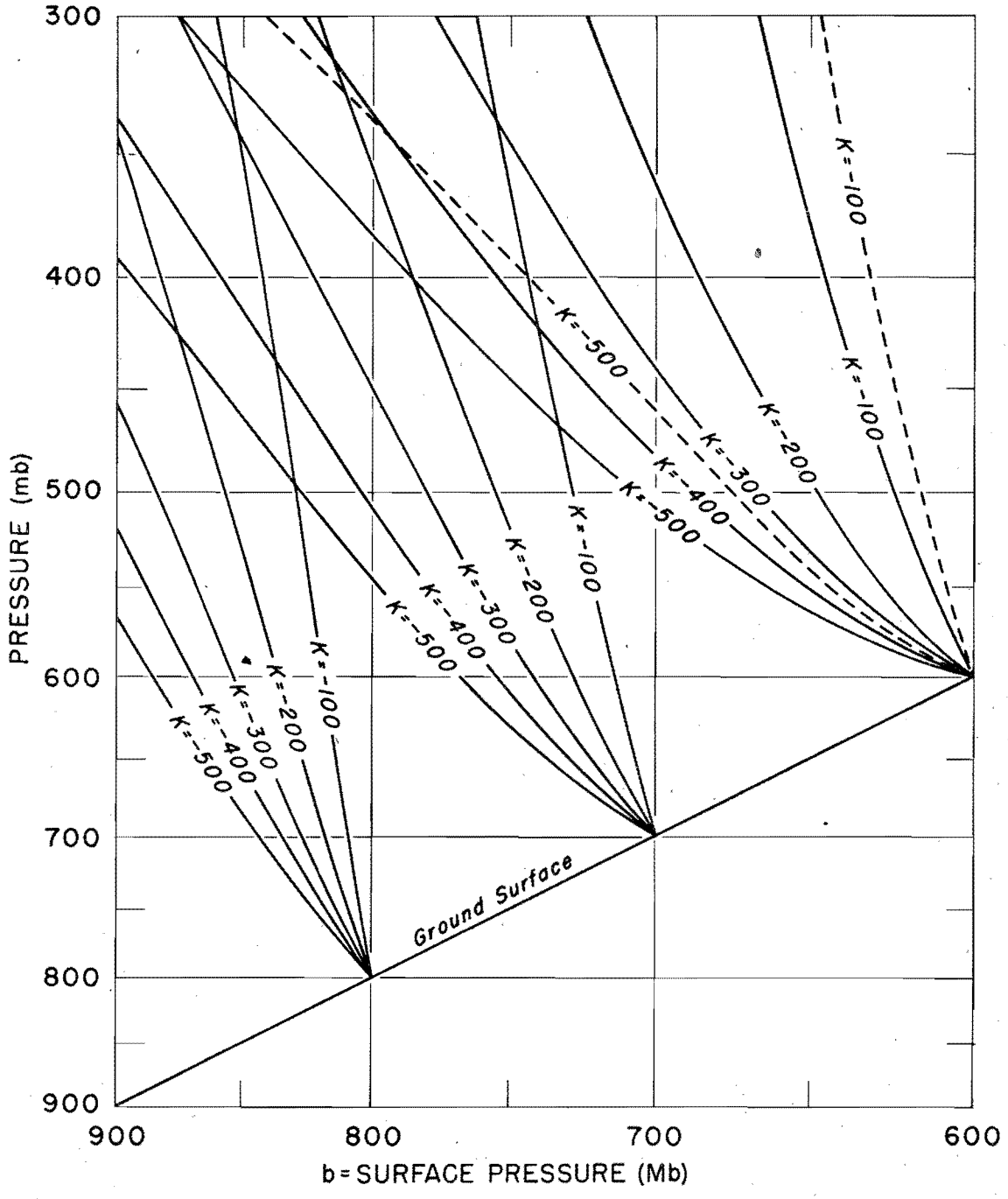

File 47002 Hydrometeorological Report 24 Figure 7

LAYERS OF EQUAL MASS TRANSPORT
San Joaquin River Basin Maximum Storm

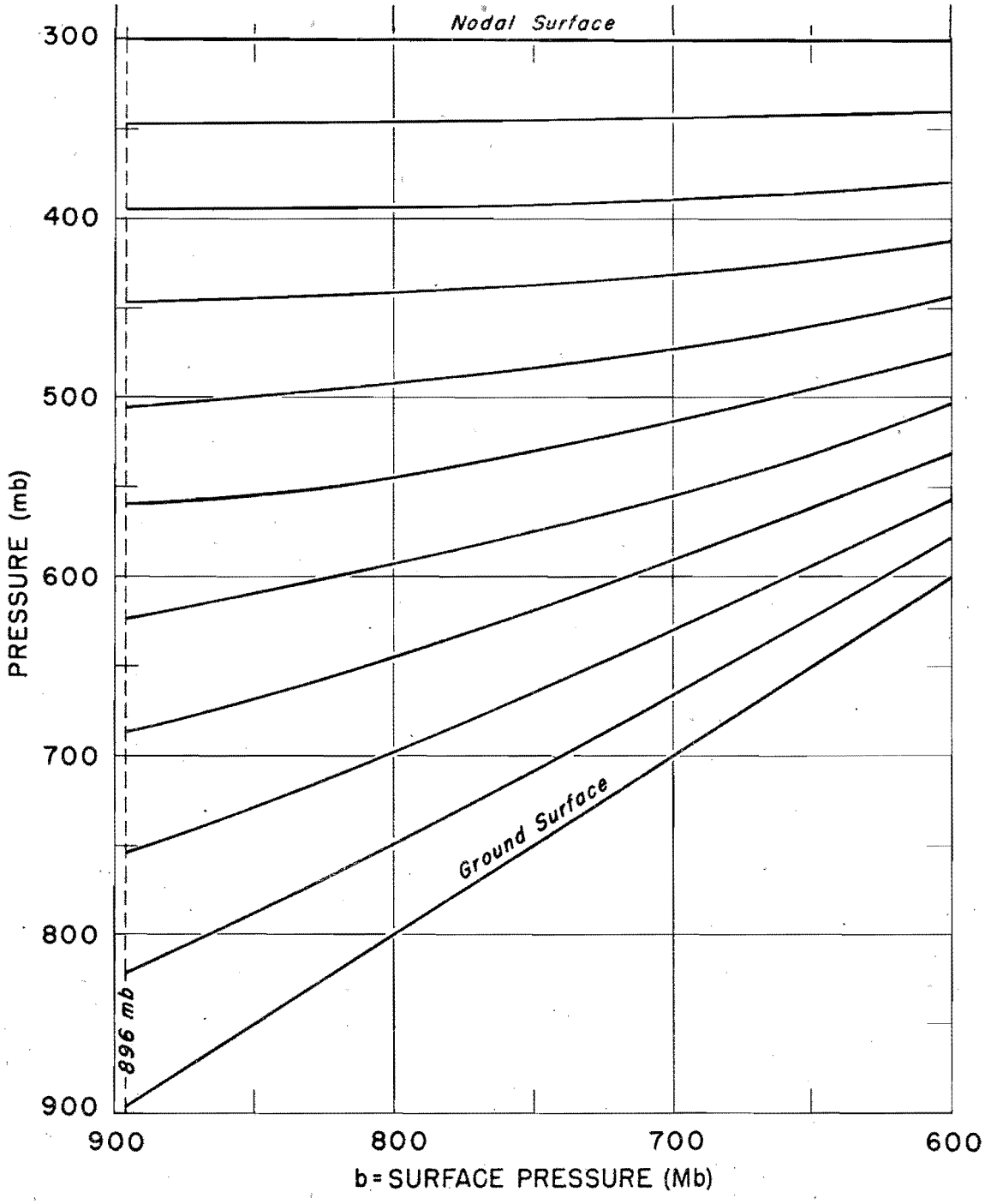

File 47002 Hydrometeorological Report 24 Figure 8

SPILLOVER-OUTFLOW CHART $\left(\frac{D_{so}}{D}\right)$

San Joaquin River Basin Maximum Storm

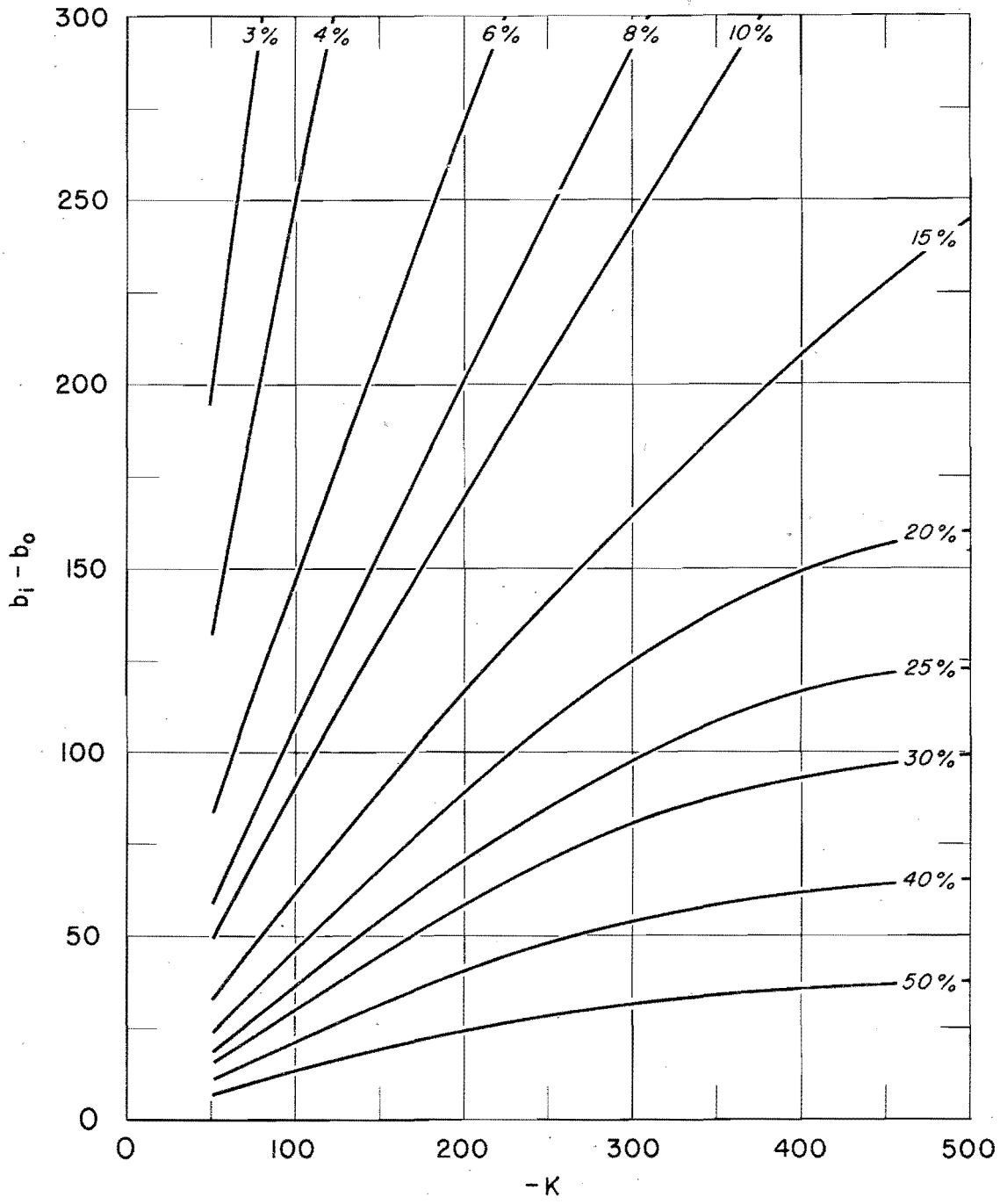

STORM PROFILES
San Joaquin River Basin

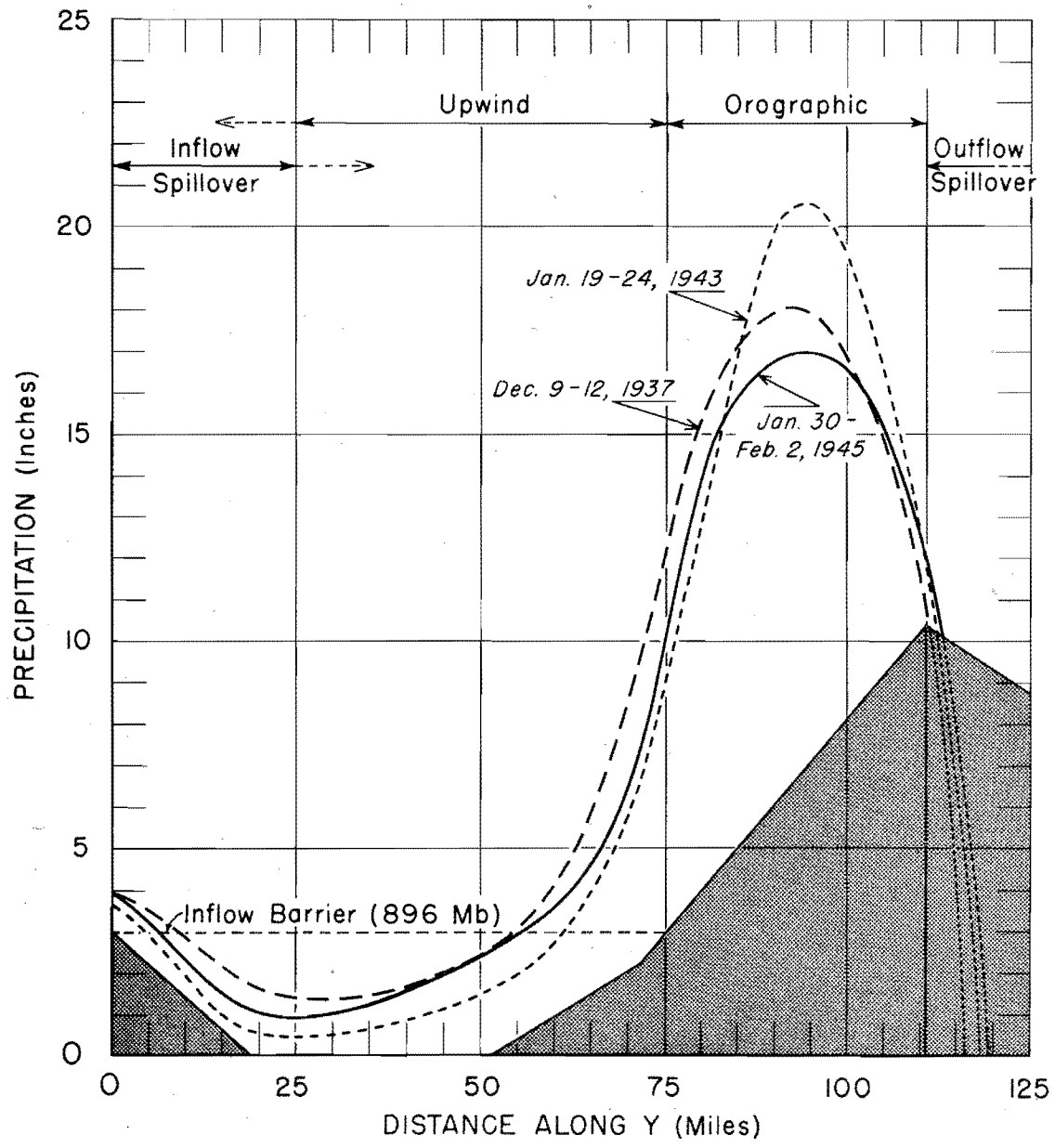

PRECIPITATION DISTRIBUTION IN MAXIMUM OROGRAPHIC STORM
(By 6 – Hour Periods)
San Joaquin River Basin

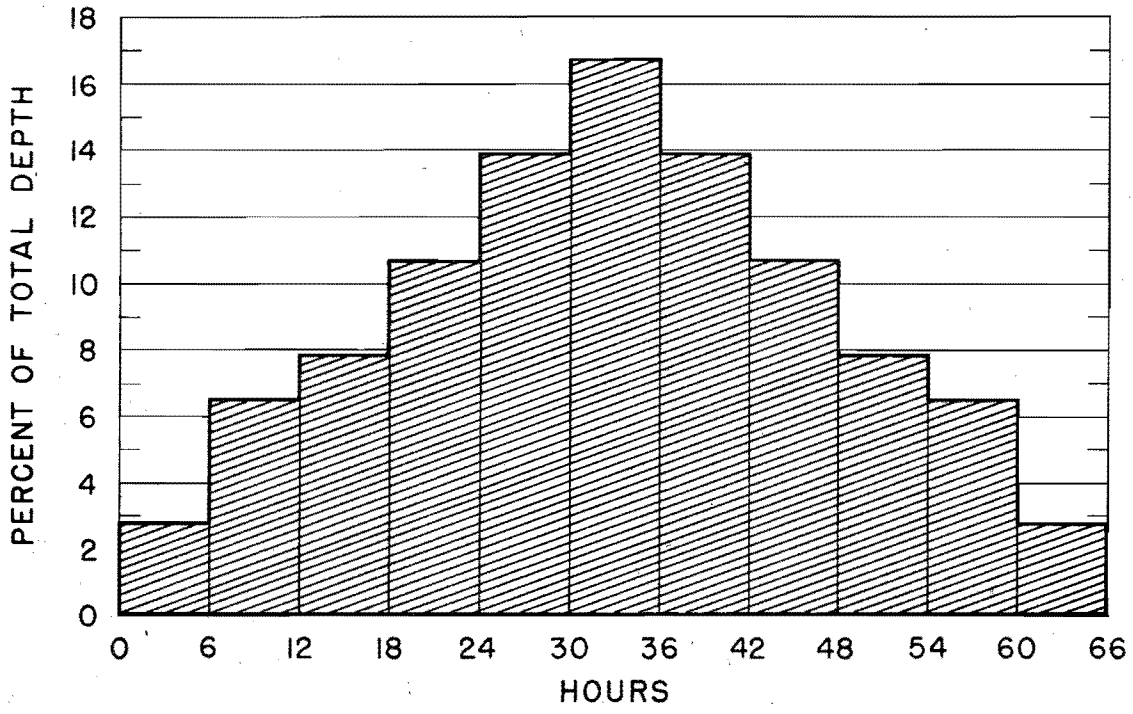

MAXIMUM POSSIBLE PRECIPITATION

Depth - Duration Curves

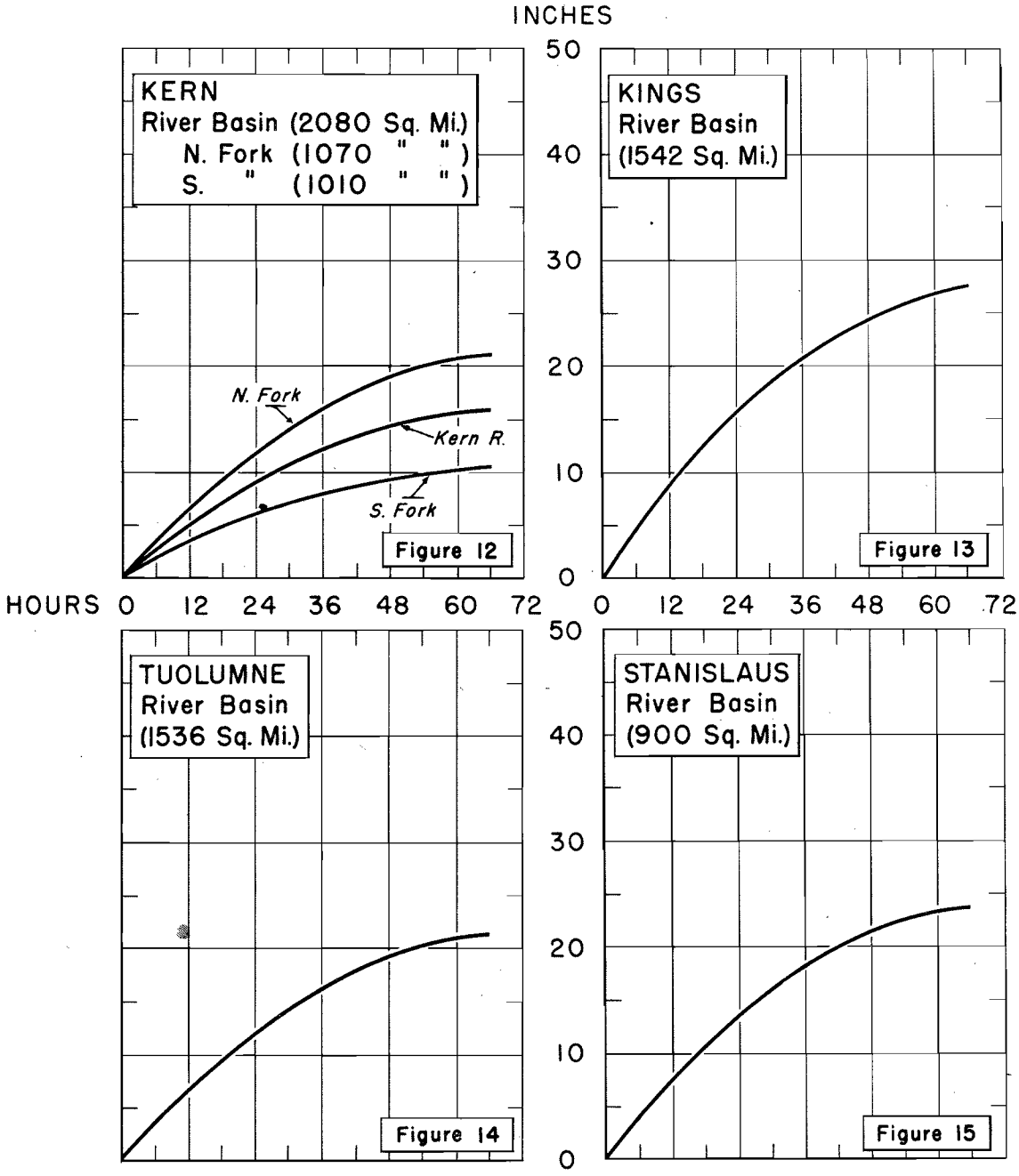

MAXIMUM POSSIBLE PRECIPITATION
Depth - Duration Curves

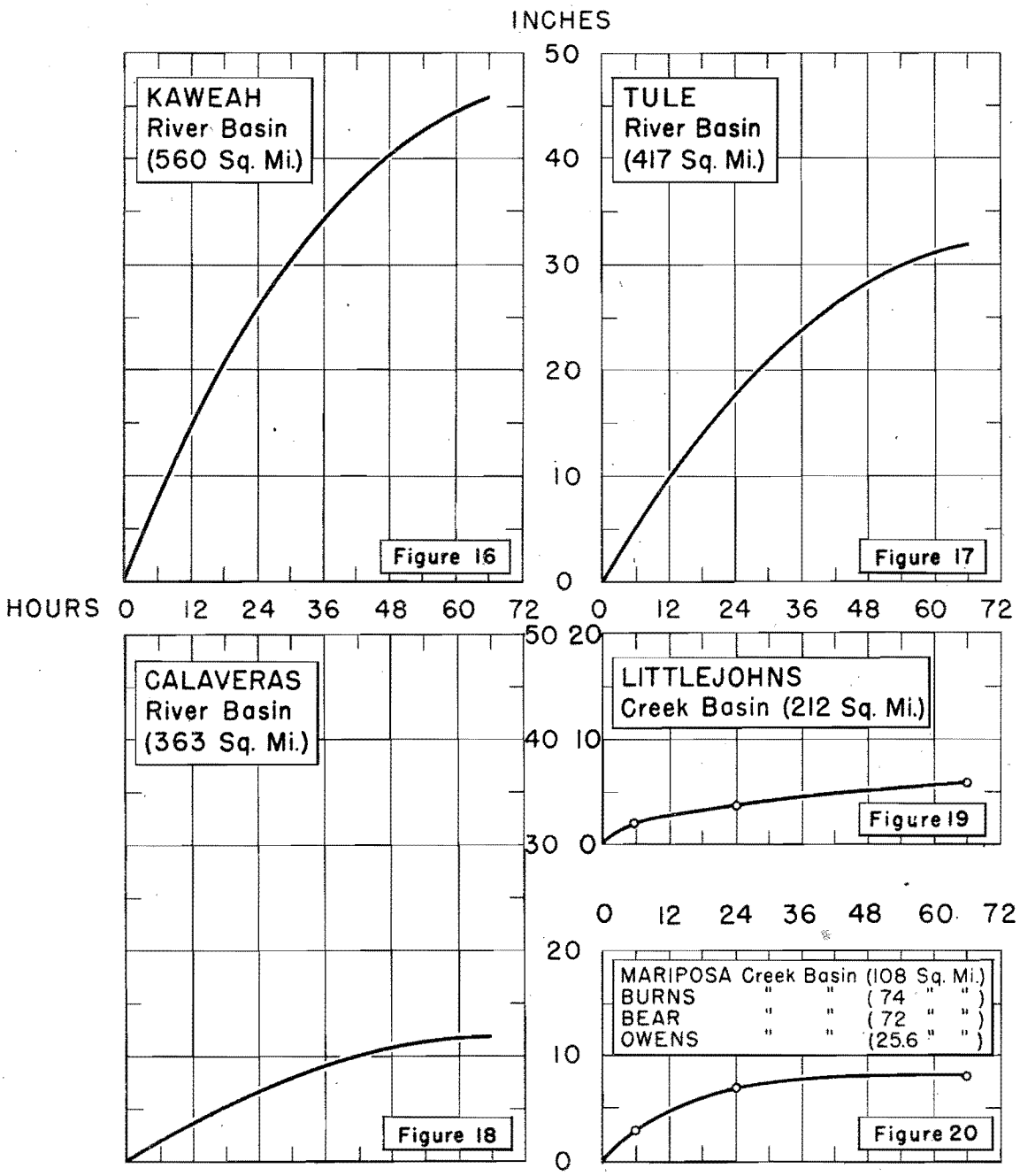

THEORETICAL RATES OF SNOW MELT DUE TO ATMOSPHERIC TURBULENCE
(Per Unit Wind Velocity)

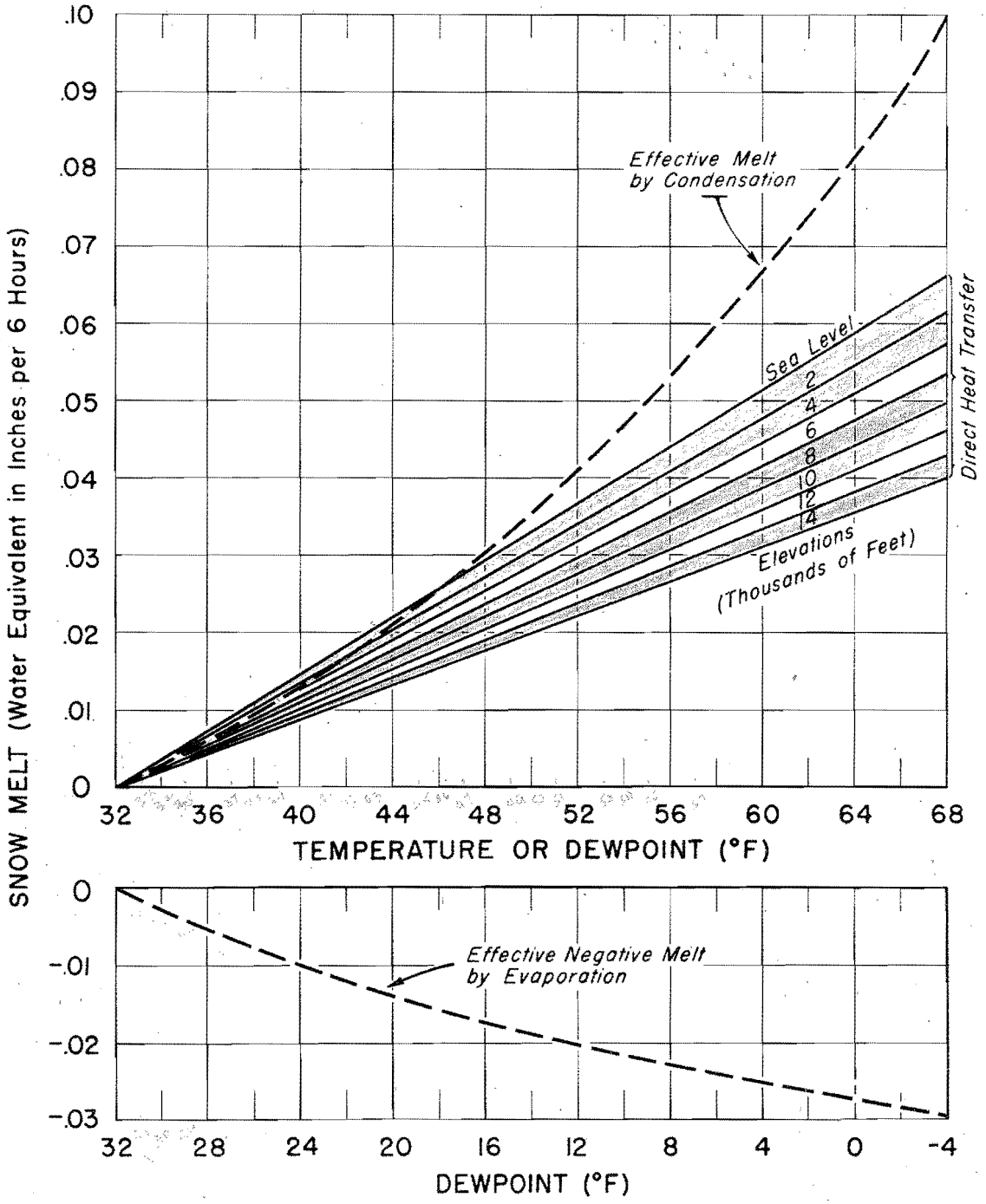

File 47002 Hydrometeorological Report 24 Figure 21

SNOW MELT DUE TO RAINFALL
With Snow Surface at 32° F

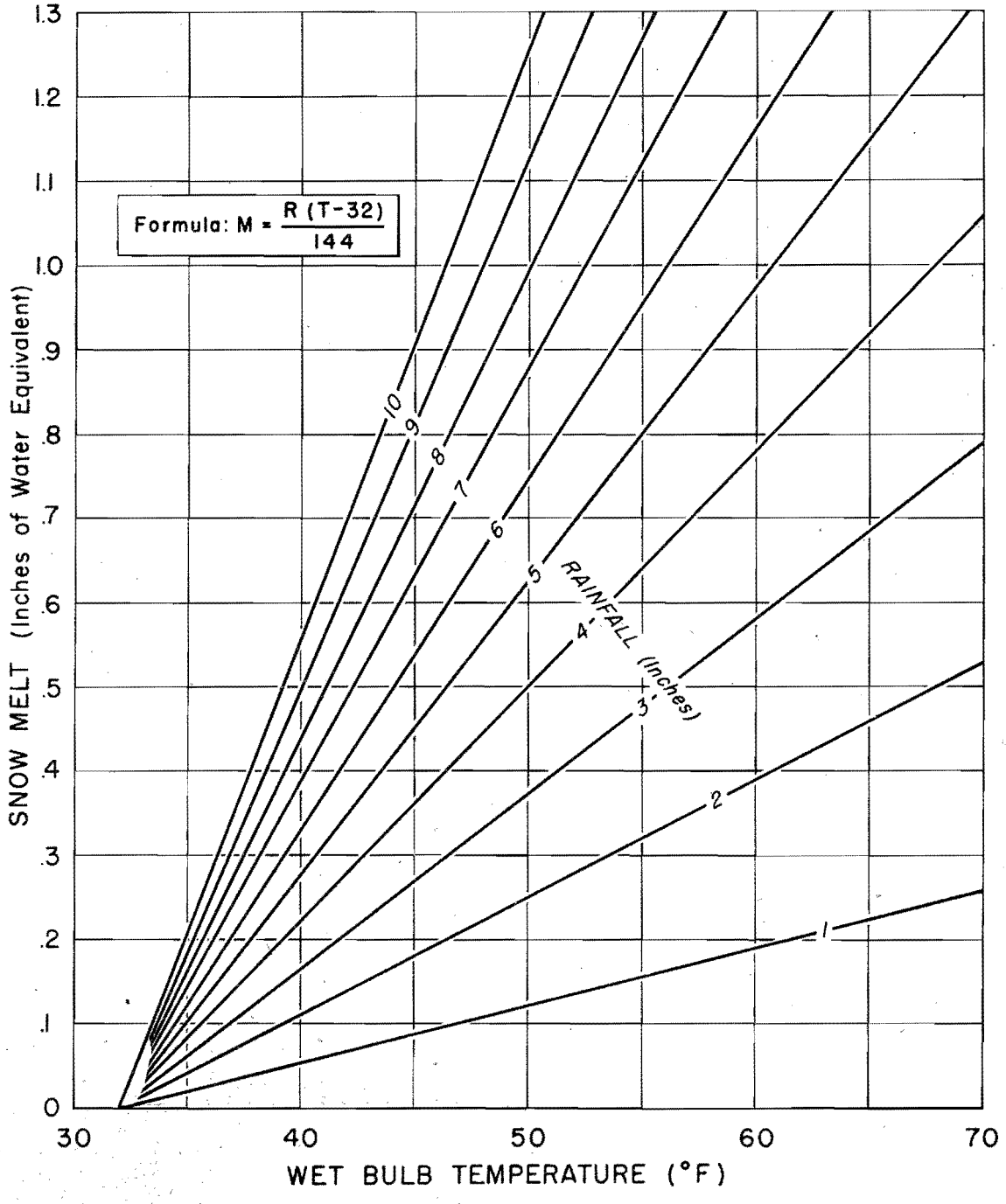

File 47002 Hydrometeorological Report 24 Figure **22**

DISAPPEARANCE OF SNOW ON GROUND
1938 Snow-Melt Season, Tuolumne River Basin

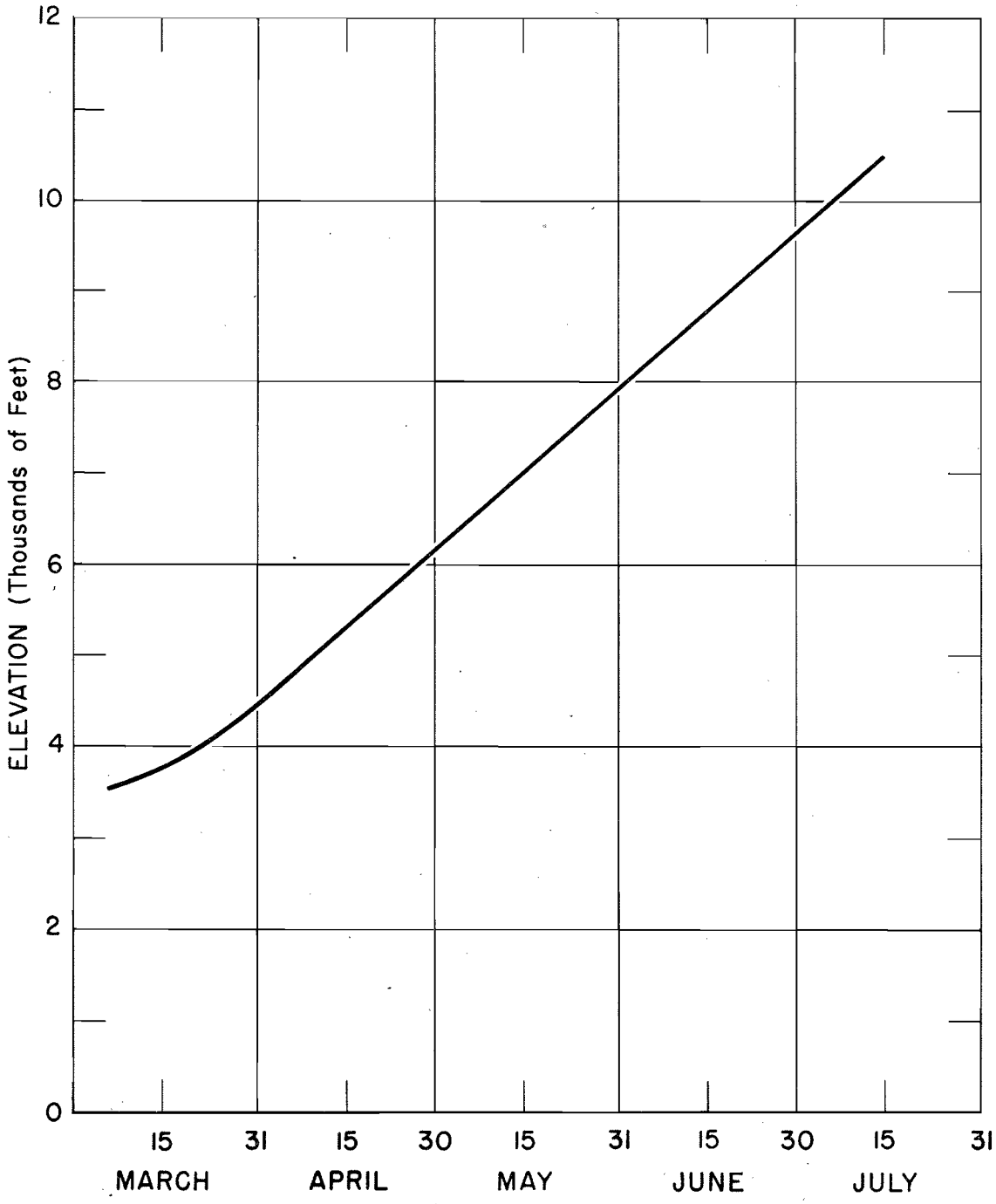

AREA-ELEVATION CURVE
Tuolumne River Basin

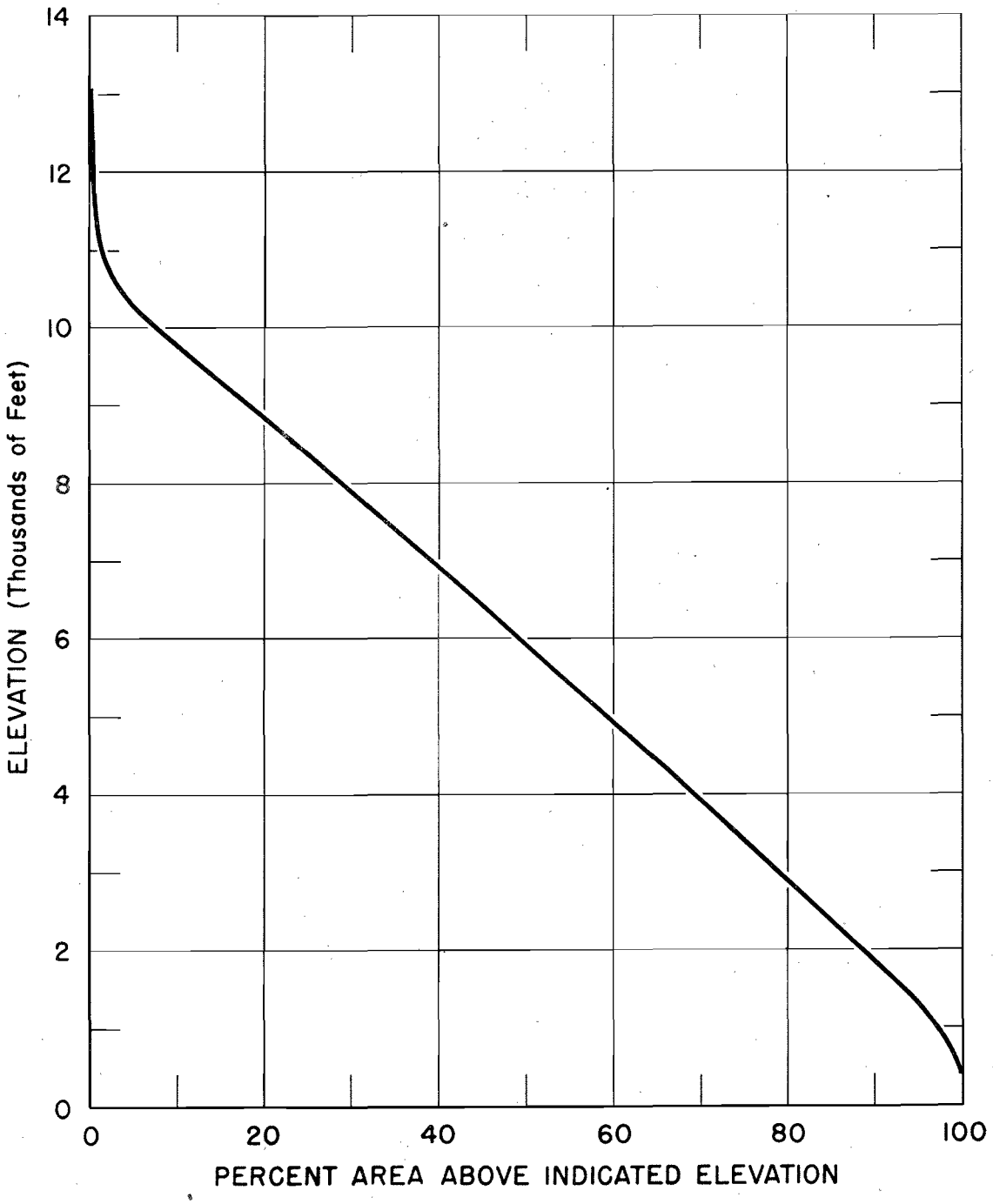

File 47002 Hydrometeorological Report 24 Figure 24

ENVELOPING SNOW DEPTH-ELEVATION CURVES
San Joaquin River Basin

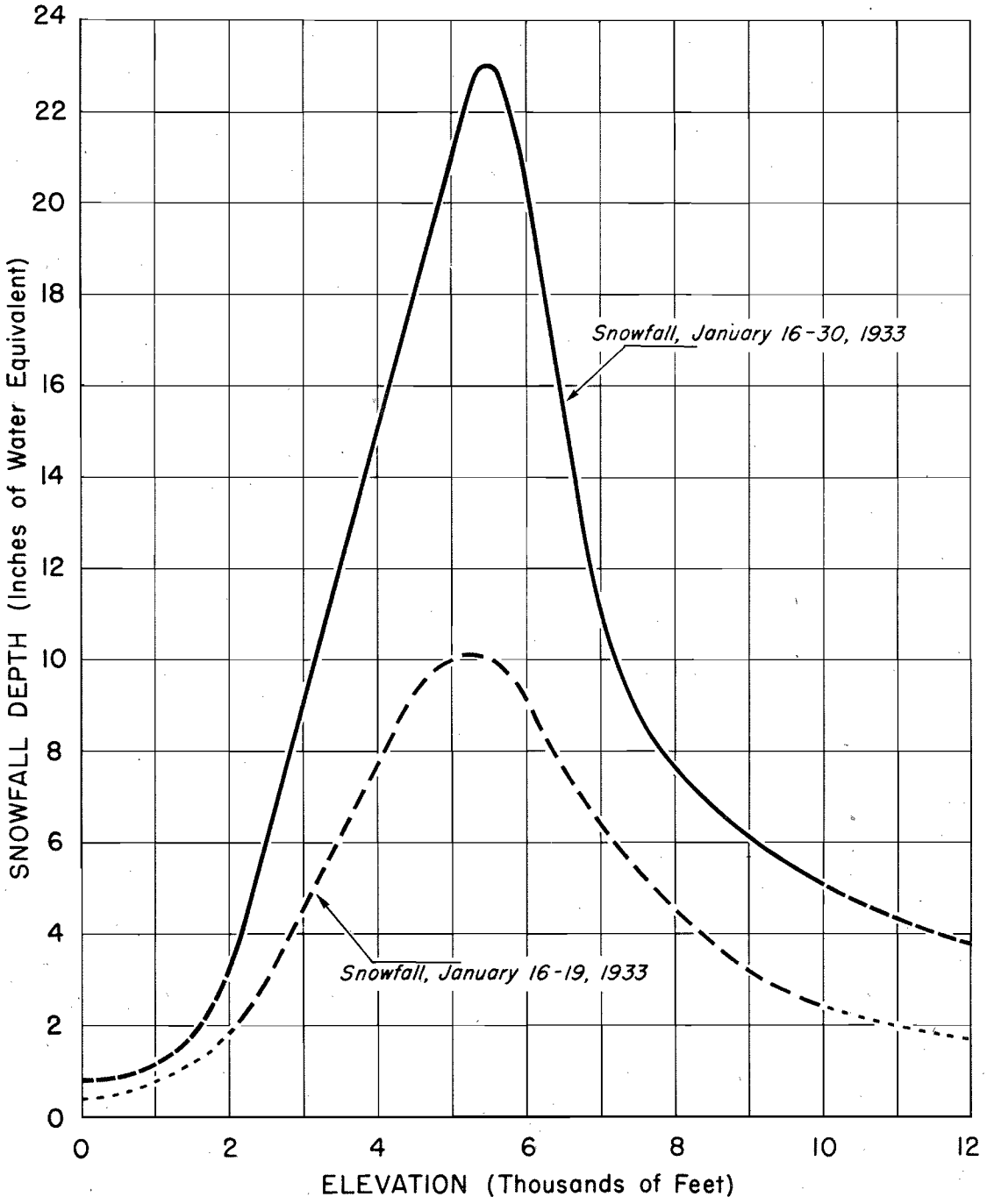

File 47002 Hydrometeorological Report 24 Figure **25**

ASSUMED METEOROLOGICAL SEQUENCE FOR COMPUTATION OF MAXIMUM SNOW MELT
San Joaquin River Basin

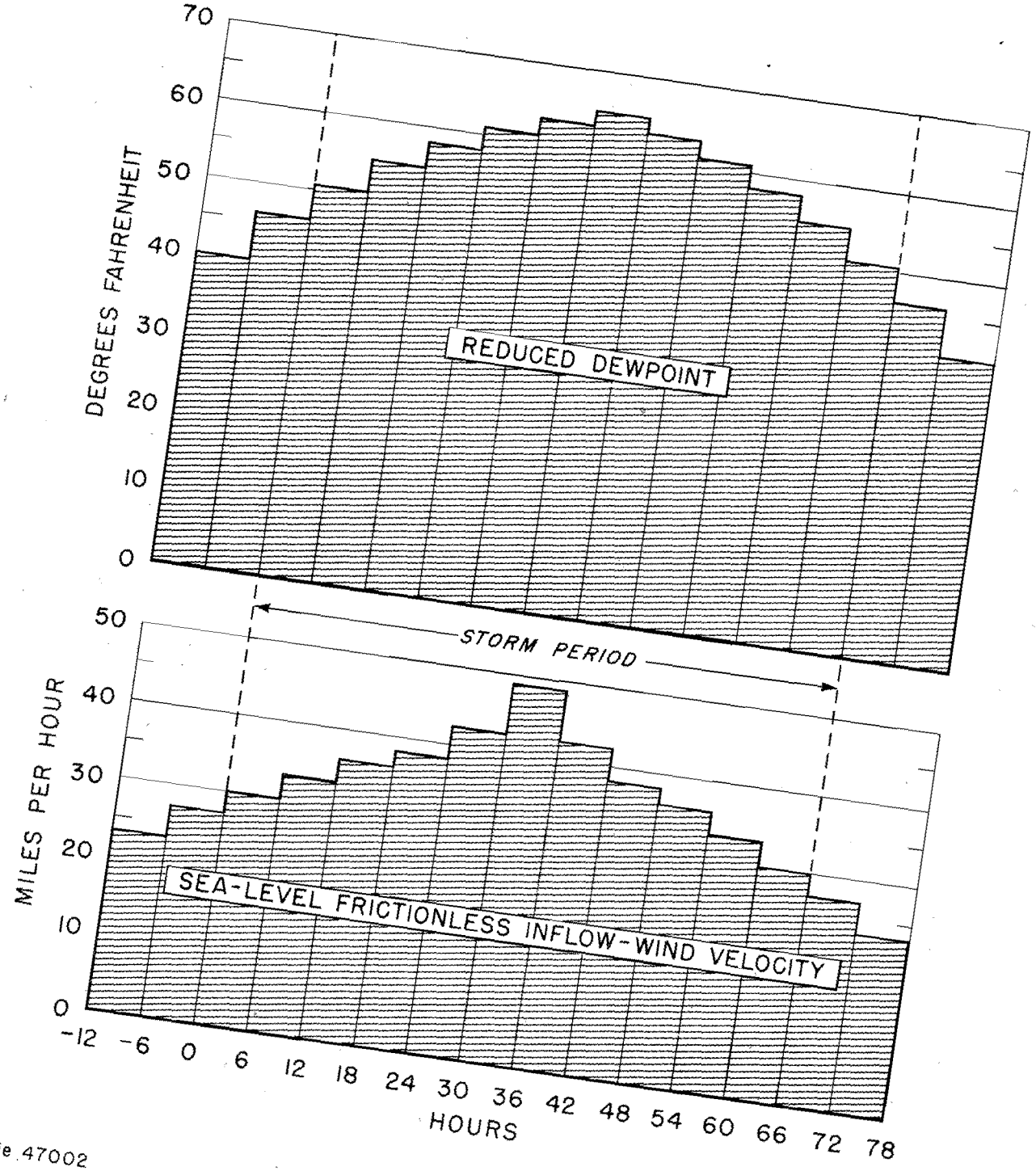

File 47002

Figure 26

VARIATION OF WIND ALONG WINDWARD SLOPES
San Joaquin River Basin

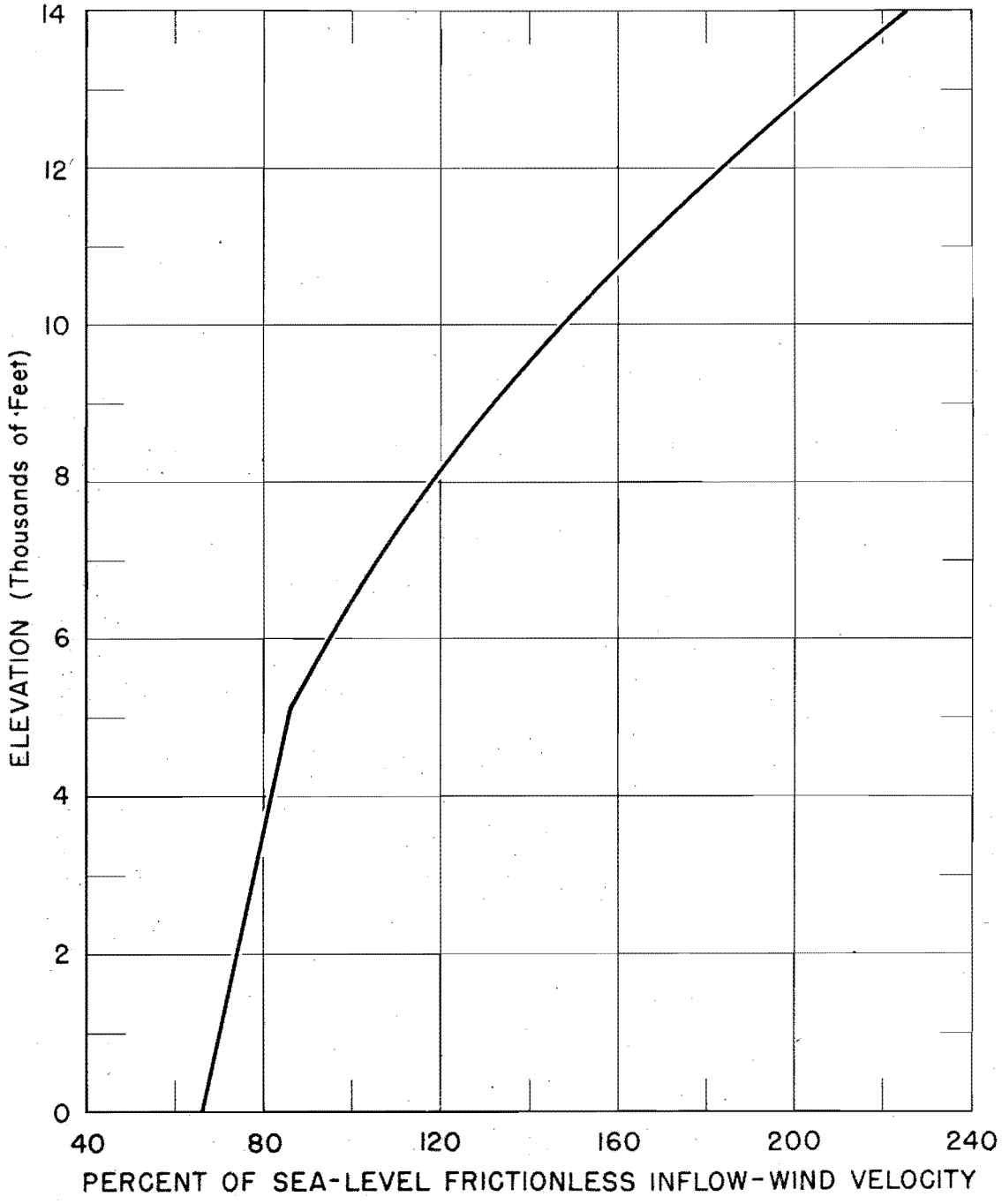

File 47002 Hydrometeorological Report 24 Figure 27

TURBULENCE SNOW MELT BY 1000-FT ELEVATION INTERVALS

(Per Unit Sea-Level Frictionless Inflow-Wind Velocity)

San Joaquin River Basin

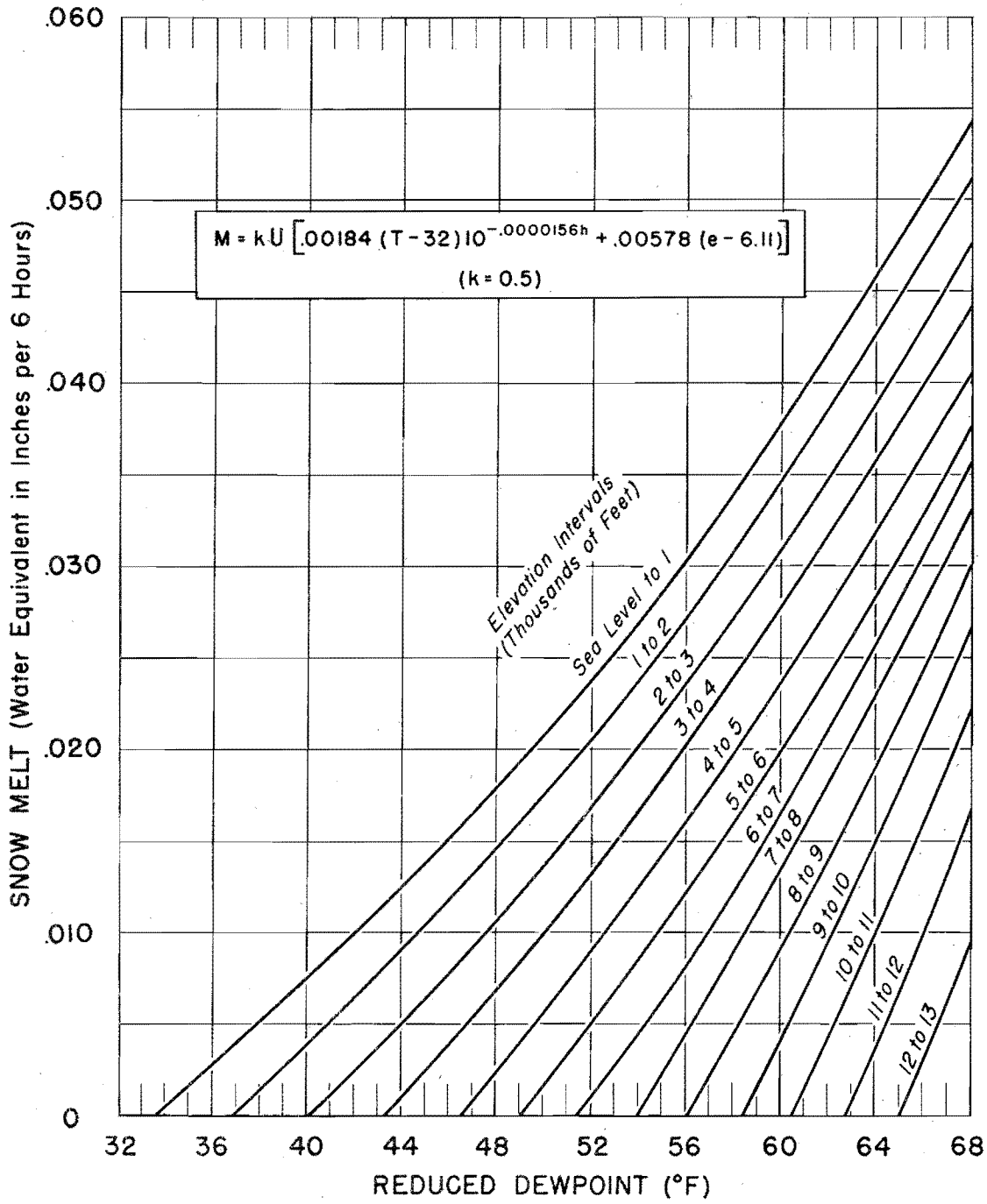

GRAPHICAL SUMMARY OF TOTAL SNOW MELT
Kings River Basin Maximum Storm

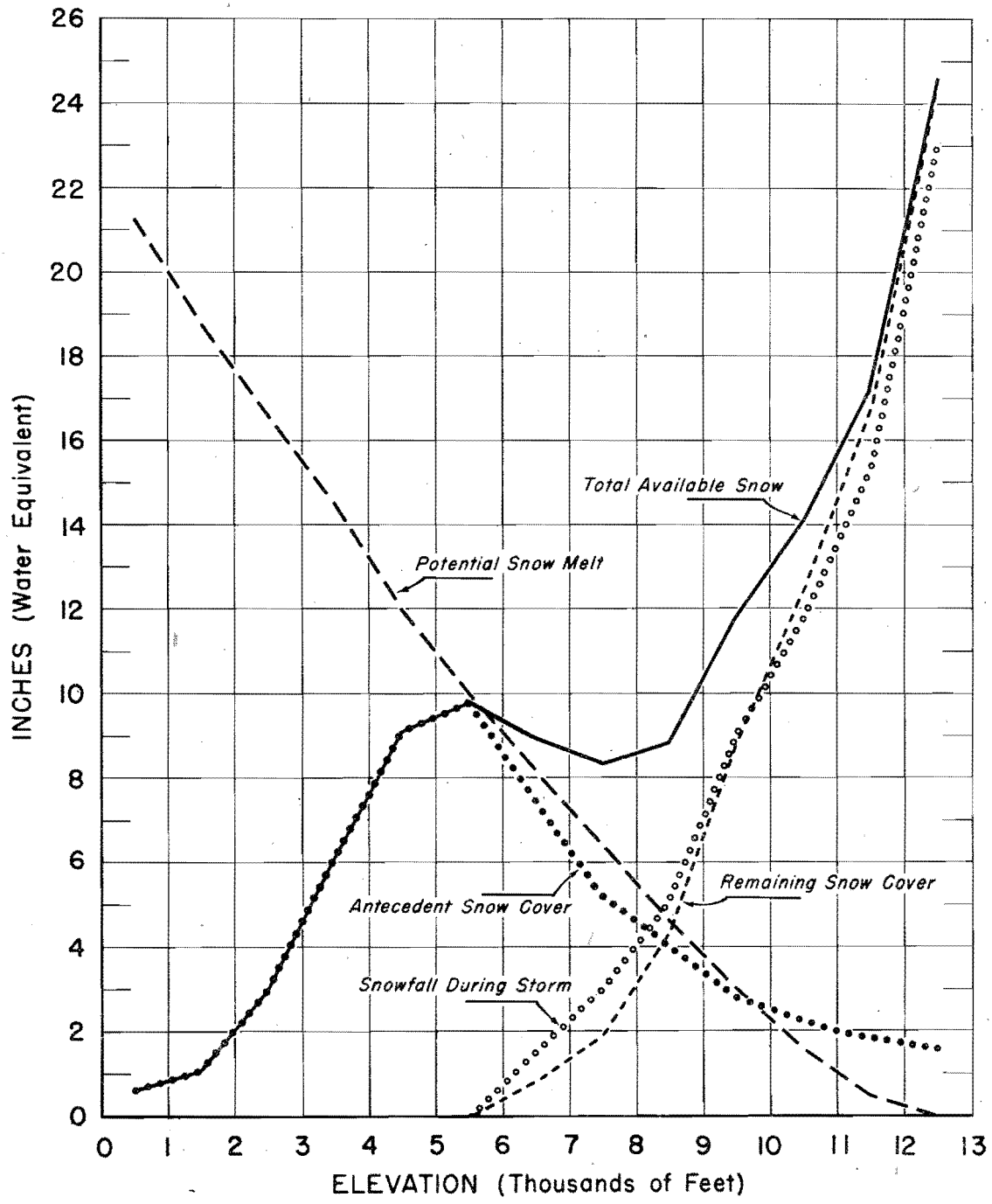

COMPARISON of CALCULATED and OBSERVED MAXIMUM PRECIPITATION

(Accumulated 6-Hour Increments, Identical 66-Hour Period)

Storm of Jan. 30-Feb. 2, 1945

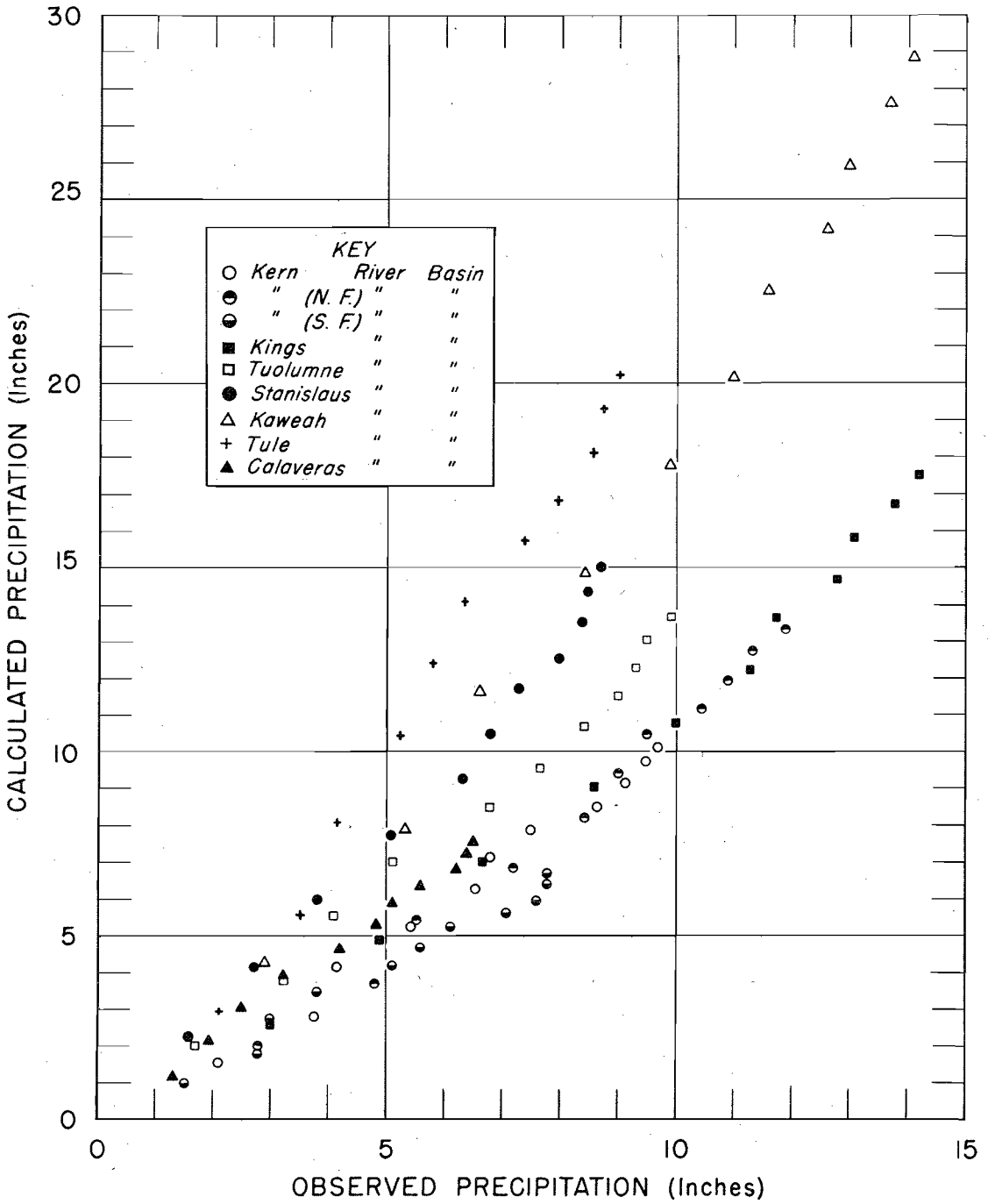

EFFECT OF INFLOW BARRIER HEIGHT ON CALCULATED-OBSERVED PRECIPITATION DIFFERENCES

Storm of Jan. 30-Feb. 2, 1945